Journal of Nanobiotechnology

RESEARCH

Open Access

m6A-modified exosome-derived circHIF1α binding to KH domain of IGF2BP3 mediates DNA damage and arrests G1/S transition phase to resists bacterial infection in bacteremia

Jiang Yu[1,2*†], Yidan Gao[1,2†], Fei Liu[1], Yuyu Zhang[1,2], Jianda Li[1], Luogang Ding[1], Sufang Ren[1], Jie Yang[1], Jian Jiao[1], Gong Feng[1], Zhi Chen[1], Wenbo Sun[1] and Jiaqiang Wu[1,2*]

Abstract

Background Animal and human health are seriously threatened by bacterial infections, which can lead to bacteremia and extremely high rates of morbidity and mortality. Recently, there have been reports indicating the involvement of exosomal circular RNAs (circRNAs) in a range of human disorders and tumor types. However, the role of exosomal circRNAs in bacterial infection remains elusive.

Methods We extracted and identified exosomes from the culture medium of PIEC cells infected with or without *Glaesserella parasuis*. RNA sequencing analysis was performed on the exosomes to screen and identify circRNAs (circHIF1α) associated with *Glaesserella parasuis* infection. PIEC cells were infected with *Staphylococcus aureus* or *Streptococcus suis* 2 to further determine whether exosome-derived circHIF1α was the crucial circHIF1α associated with bacterial infections. The transmission process of exosomes and their circHIF1α between cells was clarified via exosome tracing and co-culture assay. Moreover, the mechanism of circHIF1α being packaged into exosomes was explored, and the effects of exosomes and their circHIF1α on cell proliferation, DNA damage and cell cycle were analyzed. In addition, the binding mode and site of interacting proteins with circHIF1α were further determined. In vivo and in vitro, the role of exosomes and their circHIF1α in host resistance to bacterial infection was confirmed.

Results We first discovered a new circHIF1α that was very stable and detectable, encapsulated into exosomes by hnRNPA2B1, and whose expression in exosomes of bacterially infected PIEC cells significantly decreased. Additionally, exosomal circHIF1α reduced bacterial infection both in vitro and in vivo and suppressed the growth of reception

†Jiang Yu and Yidan Gao contributed equally to this work.

*Correspondence:
Jiang Yu
yujiang_2213@163.com
Jiaqiang Wu
wujiaqiang2000@sina.com

Full list of author information is available at the end of the article

cells. Mechanistically, the circHIF1α interacted with the KH domain of IGF2BP3 in an m6A-modified manner, which mediated DNA damage to arrest the cells at the G1/S phase through the interaction between the regulator of Chromosome Condensation 2 (RCC2) and γ-H2AX protein. Exosomal circHIF1α is a unique therapeutic target for bacterial infection since this work highlights its critical function in fighting bacterial infection.

Keywords Bacterial infection, Exosomal circHIF1α, m6A methylation, IGF2BP3, DNA damage, Cell cycle

Introduction

Bacterial infections are a major threat to human and animal health [1]. The main reason for the investigators' attention is that it could trigger inflammation in the body and cause bacteremia [2–4], which results in tremendous morbidity and mortality. Bacteremia is one type of severe infection due to the presence of pathogenic microorganisms that multiply in the blood and travel through the bloodstream to other organs [5]. To date, it is not clear how bacteremia affects the organs after bacterial infection. Moreover, the defense mechanism of organisms remains elusive. In order to increase the efficacy of treating both Gram-positive and Gram-negative bacteria, it is crucial to investigate the mechanism underlying the host's defense against bacterial infections and pinpoint therapeutic targets.

Exosomes, a diameter ranging from 40 to 160 nm (~100 nm on average) [6], containing membrane proteins, cytosolic and nuclear proteins, extracellular matrix proteins, metabolites, and nucleic acids (namely mRNA, noncoding RNA, and DNA), are important mediators of cell-to-cell information transmission [7, 8], which affect cell physiological state [9]. Emerging evidence indicates that as a special type of noncoding RNA with covalently closed single-stranded loop produced by back-splicing of precursor mRNAs that lack 5' caps and 3' poly(A) tail, circular RNAs (circRNAs), are definitively enriched in exosomes [10]. CircRNAs are highly conserved and stable compared with their linear RNAs counterparts [11]. Many studies have verified that circRNAs act as competing endogenous RNAs (ceRNAs) to mediate gene levels [12, 13]. Nevertheless, current research has shown that circRNAs bind to RNA-binding proteins and control their activity [14]. At present, circRNAs were confirmed to be closely related to disease development and progression, which mainly focused on various cancers [15, 16]. However, it is still unclear how the circRNAs function biologically in bacterial infection.

The most common methylation modification in eukaryotes, N6-methyladenosine (m6A) modification, is a crucial regulator of the synthesis and activity of mRNAs and noncoding RNAs [17–19]. Multiple studies have revealed that m6A occurs in circRNAs, and m6A modification not only contributes to the synthesis and nucleocytoplasmic transport of circRNAs but also facilitates circRNA-protein interactions [20, 21]. The interplay between m6A modification and circRNA was reported to regulate proliferation, metastasis, angiogenesis, and metabolism in a variety of cancers, including prostate cancer, cervical cancer, and so on [22, 23]. The insulin-like growth factor II mRNA binding protein 3 (IGF2BP3), as an m6A reader, interacts with circRNA to regulate cancer progression [24]. Uncertainty persists regarding the molecular mechanism behind the regulation of IGF2BP3 expression during bacterial assault.

In the present study, we choose *Staphylococcus aureus* (*S. aureus*), *Streptococcus suis* 2 (SS2), and *Glaesserella parasuis* (*G. parasuis*) as the representative bacteria, the porcine iliac artery endothelial cells (PIEC) as donor cells and porcine kidney cells (PK-15) as receptor cells were used to study the mechanism of the organism's resistance to bacteremia. We discovered a new circHIF1α that was markedly downregulated in exosomes derived from bacterially contaminated PIEC cells. Further analyses indicated that circHIF1α inhibited the proliferation of receptor cells, and exosomal circHIF1α could prevent bacterial invasion and protect the organism against bacterial infection in vitro and in vivo. Mechanistically, the circHIF1α directly bound to the KH domain of IGF2BP3 in an m6A-mediated manner and enhanced the stability of IGF2BP3, which mediated DNA damage and modulated G1/S transition of the cell cycle of receptor cells in the interaction between the regulator of Chromosome Condensation 2 (RCC2) and γ-H2AX protein. According to this study, a novel therapeutic target for bacterial infection is exosomal circHIF1α.

Materials and methods

Bacterial strains and cell culture

G. parasuis serovar 5 stain LZ, SS2 strain QH, and *S. aureus* ATCC29213 were preserved in our laboratory. *G. parasuis* was grown on Trypticase Soy Agar (TSA) or Trypticase Soy Broth (TSB) (OXOID, Basingstoke, UK) with the addition of 0.01% nicotinamide adenine dinucleotide (NAD) and 5% (v/v) inactivated bovine serum at 37 °C. SS2 was cultured on TSA or TSB with 5% (v/v) inactivated bovine serum at 37 °C. *S. aureus* was grown on Luria Broth medium.

PIEC cells and PK-15 cells were preserved in our laboratory. PIEC cells were cultured in RPMI-1640 medium (Gibco, Carlsbad, USA) supplemented with 10% fetal bovine serum (FBS) (Gibco, Carlsbad, USA), and PK-15 cells were cultured in DMEM medium (Gibco, Carlsbad, USA) supplemented with 10% FBS, 100 mg/mL

streptomycin and 100 U/mL penicillin. All these cells were maintained in a humidified incubator at 37 °C with 5% CO_2.

Exosomes isolation

Ultracentrifugation is the gold standard for exosome isolation [25]. Exosomes were isolated from the supernatant of PIEC culture with exosome-depleted medium following the improved method according to the ultracentrifugation steps reported [26, 27]. Briefly, centrifugation at 500 × g for 5 min to remove cells from the samples, transferring the supernatant to a new polycarbonate tube and centrifuging 10 min at 2000 × g. The supernatant was collected and transferred to a new polycarbonate tube. Then, centrifugation for 30 min at 10,000 × g to eliminate shed microvesicles (sMV, 200–1000 nm). The supernatant was collected and filtered with 0.22 μm membrane filter (Merck Millipore, Darmstadt, Germany) and further centrifuged at 100,000 × g for 2 h at 4 °C twice to pellet the exosomes. Finally, exosomes were resuspended in 50 μl to 100 μl phosphate-buffered saline (PBS) and stored at -80 °C for further use.

Exosome identification and internalization

The 50 μl exosome samples were loaded into nanoscale bronze grating after negative staining by uranyl acetate, and the shape and size of the exosomes were observed by transmission electron microscopy (TEM) (Tecnai G2, FEI, USA) at 120 kV. The size distribution of the exosomes was characterized using a Nanosight NS300 (NanoSight Ltd., Amesbury, UK) equipped with a 405 nm laser to determine the size and quantity of particles isolated. A video of 60s duration was taken with a frame rate of 30 frames/s, and particle movement was analyzed using NTA software (version 2.3; NanoSight Ltd.). The concentration of exosomal proteins was analyzed indirectly with the BCA Protein Assay Kit (Thermo Fisher Scientific, USA), and exosomal protein markers CD63 (ABclonal, Wuhan, China), HSP70 (Proteintech, Chicago, USA) and negative marker for exosome purity Calnexin (Proteintech, Chicago, USA) were detected by Western blot. The green fluorescent dye PKH67 (Sigma, St.Louis, USA) was utilized to label exosomes isolated from the culture medium of PIEC cells. After recipient PK-15 cells were incubated with the dye for 12 h, laser confocal microscopy (Leica, SP8, Germany) was performed to visualize PKH67-labelled exosomes in PK-15 cells. The detailed procedures were performed according to the previous report [10].

Cell treatment to inhibit exosome secretion

A pharmacological inhibitor of neutral sphingomyelinase-2 (nSMase) GW4869 could reduced ceramide formation [28]. 20μM GW4869 (MCE, New Jersey, USA) was used to treat PIEC cells for 2 h to block exosome formation, and exosomes were isolated. The content of C24:1 Ceramide (d18:1/24:1(15Z))(aladdin, Shanghai, China) in exosomes was analyzed by High-performance LC/MS to confirm that the secretion of exosomes by PIEC cells was reduced after GW4869 treatment according to the previous report [28]. At the same time, the level of exosome-derived circHIF1α was analysed by qRT-PCR.

CircRNA sequencing and analysis

Total RNAs of PIEC cells and PIEC cells infected with *G. parasuis* were extracted with TRIzol reagent (Invitrogen, Carlsbad, USA) and quantified by the NanoDrop ND-1000 (Thermo Fisher Scientific, Waltham, USA), then 1–2 g total RNA from each sample was selected for RNA sequencing library construction. Image analysis and base calling were performed using Solexa pipeline v1.8 (Off-Line Base Caller software, v1.8). Sequence quality was examined using the FastQC software (v0.11.7). The trimmed reads (trimmed 5', 3'-adaptor bases using Cutadapt (v1.17)) were aligned to the reference genome using Star software. Back splice junction Reads detection and Reads count statistics were carried out by CIRCexplorer 2. The differential expression was calculated by R software edgeR. PCA analysis and correlation analysis based on gene expression level, and further data mining analysis such as clustering of differentially expressed genes, GO function significance enrichment analysis, pathway significance enrichment analysis, and so on were completed by the custom program (python/R/shell) of KangCheng Bio-tech (Shanghai, China).

Quantitative real-time PCR (qRT-PCR)

Total RNA was extracted using a TRIzol reagent. RNA concentration was measured by NanoDrop 2000. The total RNA was synthesized into cDNA with PrimeScript RT Reagent Kit (Takara, Dalian, China) in accordance with the manufacturer's protocols. The cDNA was amplified with TB Green Premix Ex Taq (Takara, Dalian, China) on a Bio-Rad CFX96 system (Bio-Rad, CA, USA). The expression of circRNAs and mRNA was determined by $2^{-\Delta\Delta CT}$ and normalized by Glyceraldehyde 3-phosphate dehydrogenase (GAPDH) or β-actin. The primers in the study were listed in Table S1.

RNase R treatment

Total RNA (2 μg) was incubated for 30 min at 37 °C with or without 3 U/μg RNase R (Geneseed, Guangzhou, China), followed by qRT-PCR analysis.

Actinomycin D assay

PIEC cells were transferred to 24-well plates, exposed to 2 μg/ml actinomycin D (MCE, New Jersey, USA) and

collected at the indicated time points. The stability of circRNA and their mRNA was analysed by qRT-PCR.

Isolation of cytoplasmic and nuclear fractionation

PIEC cells were harvested and treated using a Cytoplasmic & Nuclear RNA Purification Kit (Norgen Biotek, Canada) according to the manufacturer's instructions. β-actin and U6 served as controls of cytoplasmic RNA and nuclear RNA, respectively. The expression of circRNA, β-actin, and U6 was determined by qRT-PCR. The primers are listed in Table S1.

Co-culture assay

A total of 2.5×10^5 PIEC cells were seeded in the upper chamber of the transwell membrane (Corning, USA), and 5×10^5 PK-15 cells were seeded in the lower chamber. The upper PIEC cells were infected by *G. parasuis* (MOI = 10) and then cultured at 37 °C with 5% CO_2 for 12 and 24 h, respectively. The qRT-PCR technology was used to detect the changes of circHIF1α in upper cells (PIEC) and lower cells (PK-15) and their supernatants, respectively.

Plasmid, siRNAs, and cell transfection

The full length of the liner sequence of circHIF1α was amplified and subcloned into the lentiviral vector pLC5-ciR (Geneseed, Guangzhou, China) to construct circHIF1α overexpression vector, named ov-circHIF1α. Two siRNAs targeting circHIF1α (si-circHIF1α), two siRNAs targeting IGF2BP3 (si-circHIF1α), and negative control (si-NC) were synthesized by Boshang (Jinan, China). FLAG-tagged expression pcDNA3.1 vectors for full-length swine IGF2BP3 and site-directed mutants were provided by Boshang (Jinan, China). Full-length circHIF1α and its truncations were subcloned into pcDNA3.1 (Boshang, Jinan, China). Cellular transfection of siRNA and plasmid was conducted using Lipofectamine™ RNAiMAX Transfection Reagent (Invitrogen, Carlsbad, USA) and Lipofectamine™ 3000 kit (Invitrogen, Carlsbad, USA) according to the manufacturer's instructions, respectively. The detailed oligonucleotide sequences used in this study are shown in Table S2, and the detailed source information for all plasmids is listed in Table S3.

Cell proliferation and cell cycle assays

The growth curves of PK-15 cells treated in 12, 24, 36, and 48 h were obtained using Cell Counting Kit-8 (Beyotime, Shanghai, China) according to the protocols of the manufacturer. For the EdU assay kit (Beyotime, Shanghai, China), the cells were incubated with 1 × EdU working solution at 37 °C for 2 h, and then subsequent staining and visualization were carried out in accordance with the manufacturer's instructions. The cell proliferation rate was calculated by the ratio of EdU-positive cells (red) to DAPI-positive cells (blue). PK-15 cells were collected and fixed in 70% cold ethanol overnight at 4 °C. Cell cycle distribution was performed using a flow cytometer (LSR Fortessa, BD, USA) after cells were treated with propidium iodide (PI, 50 μg/mL) and RNase A (100 μg/mL). Data were analyzed using ModFit LT 5.0.

RNA pulldown assay

The full length of circHIF1a was constructed on pCNDA3.1 vector and digested with FastDigest BamH I (Thermo Fisher Scientific, Waltham, USA), and then transcribed in vitro with MEGAscript RNA T7 Transcription Kit (Invitrogen, Carlsbad, USA). The probe was prepared by linking biotin with biotin 3' End Desthiobiotinylation Kit (Thermo Fisher Scientific, Waltham, USA) according to the manufacturer's instructions. RNA pulldown assay was carried out with Pierce™ RNA 3' End Desthiobiotinylation Kit (Thermo Fisher Scientific, Waltham, USA). The recovered protein was verified by Western blot or mass spectrometry assays.

RNA immunoprecipitation (RIP) assay

The RIP assay was performed with PureBinding®RNA Immunoprecipitation Kit (Geneseed, Guangzhou, China) to determine the interaction between circHIF1α and its interacting proteins. Briefly, 2×10^7 cells were harvested and lysed by RIP lysis buffer, then incubated with magnetic beads conjugated with antibodies against IgG (Cell Signaling Technology, Beverly, USA). The coprecipitated RNAs were examined using qRT-PCR with specific primers.

Methylated RNA immunoprecipitation (MeRIP) assay

The Methylated RNA Immunoprecipitation Kit (BersinBio, Guangzhou, China) was utilized to examine the m6A modifications on circHIF1α on the basis of the manufacturer's instructions. Briefly, the total RNA was extracted by Trizol reagent after collecting 2×10^7 PK-15 cells. The extracted RNA fragments were transformed into about 100 nt lengths, and then 6% RNA was used as the input group. The remaining RNA was divided into two groups and incubated with m^6A antibody and IgG antibody at 4 °C for 4 h, respectively. Protein A/G magnetic beads were added to incubate with antibody at 4 °C for 1 h. The enriched RNA was extracted and detected by qRT-PCR.

Fluorescence in situ hybridization (FISH) and immunofluorescence (IF)

A FAM-marked probe of circHIF1α was synthesized by BersinBio Company (Guangzhou, China). For the FISH assay, RNA-FISH was carried out by using a FISH Kit (RiboBio, Guangzhou, China) according to the manufacturer's protocols to assess the location of circHIF1α in PIEC cells and PK-15 cells. In the immunofluorescence

assay, PK-15 cells were transiently transfected with Cy3-labelled circHIF1α and proceeded to FISH assay, and then incubated with anti-IGF2BP3 antibody (Proteintech, Chicago, USA) to observe the colocalization of circHIF1α and IGF2BP3. All images were observed using laser confocal microscopy (ZEISS, LSM800, Germany).

Dual-luciferase reporter assay

The plasmids (pmiRGLO-WT-HIF1α and pmiRGLO-MUT-HIF1α) were synthesized and sequenced by Shandong Gene & Bio Co, Ltd (China). PK-15 cells were transfected with plasmids. After 24 h of incubation, the cells were analyzed with the Dualucif®Firefly & Renilla Assay Kit (UElandy, Shanghai, China) according to the manufacturer's instructions. Detailed source information for vectors is available in Table S3.

Western blot analysis

Total proteins of exosomes and PK-15 cells were extracted with RIPA lysis buffer containing PMSF. The protein concentration was measured by the BCA method. After being purified and electrophoretically separated, proteins were transferred to PVDF membranes (Millipore, Billerica, USA). The membranes were blocked with 5% skimmed milk for 1 h and then incubated overnight at 4 °C with each primary antibody and subsequently incubated with HRP-conjugated secondary antibodies at room temperature for 1 h. Finally, the enhanced chemiluminescence system (BeyoECL Moon, Beyotime, Jiangsu, China) was applied for signal visualization. Gray values of protein bands were quantified by Image J software. All antibodies of Western blot used in this study were listed in Table S4.

Co-immunoprecipitation (CoIP)

PMSF was added in 400 μL lysate containing 3 mg total protein, and 4 μg specific antibody was added at the same time. Moreover, an equal amount of homotypic IgG antibodies was added to an equal amount of protein lysates, which was the IgG control group. All samples were mixed overnight at 4 °C. Then 50 μl suspended ProteinA agarose beads were added and incubated at 4 °C for 4 h. The precipitated complex was washed 5 times with 1mL 1 × TBST added with PMSF. Finally, the proteins were detected by Western blot.

Bacteria adhesion and invasion assays

Adhesion and invasion assays were performed using PK-15 cells. A total of 5×10^5 PK-15 cells were cultured overnight at 37 °C with 5% CO_2 and then infected with different bacteria to allow bacterial adhesion. In this study, PK-15 cells were infected with *S. aureus* (MOI=1) for 4 h, SS2 (MOI=10) for 8 h, and *G. parasuis* (MOI=10) for 12 h, respectively. Cells were rigorously washed five times with PBS to eliminate non-specific bacterial attachment and then incubated for 10 min at 37 °C with 100 μl 0.25% trypsin-EDTA. After incubation, 900 μl ice-cold PBS was added, and cells were removed from the culture plates by scraping the bottom of the well with a sterile scalpel blade. The cell suspensions with adherent bacteria were diluted and put onto the related plates containing NAD and serum. For the bacteria invasion assay, DMEM containing 100 μg/mL gentamicin was added to the PK-15 cells cultured, which were washed twice with PBS. The cells were further incubated for 30 min to confirm that extracellular bacteria were killed. Monolayers were washed three times with PBS and intracellular bacteria were harvested as above. All of the above assays were performed in triplicate and replicated three times.

NSC 80467 (MCE, New Jersey, USA) is a DNA damaging agent that induces markers of DNA damage γ-H2AX. Thymidine (MCE, New Jersey, USA) is a DNA synthesis inhibitor that arrest the cell at the G1/S boundary prior to DNA replication. Herein, NSC 80,467 or Thymidine was used to treat the PK-15 cells after siRNAs targeting circHIF1α were transfected into PK-15 cells, then PK-15 cells infected with different bacteria (*S. aureus*, SS2 or *G. parasuis*) and the number of PK-15 cells adhered and invaded by bacteria according to the above operation method, respectively.

Animal challenge

All animal experiments were approved by the Animal Experimental Ethical Inspection Form of the Institute of Animal Science and Veterinary Medicine, Shandong Academy of Agricultural Sciences (IASVM-2022-012). 6–8 weeks old female BALB/c nude mice were obtained from Jinan Pengyue Laboratory Animal Breeding CO., Ltd. (Shandong, China). In order to determine the resistance of exosomes derived from PIEC cells to bacterial infection in animals, PIEC cells were infected with different bacteria (*G. parasuis*, SS2, and *S. aureus*) respectively. Then, the exosomes derived from PIEC cells infected with different bacteria were isolated. The exosomes of different concentrations (10 mg/kg, 20 mg/kg, and 30 mg/kg) were injected through the tail vein of mice ($n=6$ for each group). The distribution of exosomes in mice at different times after injection was observed using Bioluminescence imaging (Tanon, Shanghai, China).

To clarify the effects of exosomes and circHIF1α on bacterial infection, exosomes labeled with DiR (MedChemExpress, New Jersey, USA) were injected according to the method described above ($n=6$ mice/group), and PK-15 cells with overexpression of circHIF1α or their empty vectors were injected through the tail vein of mice ($n=6$ mice/group). After 24 h, control mice and mice injected exosome or circHIF1α were challenged with different bacteria (*G. parasuis*, SS2 or *S. aureus*) by

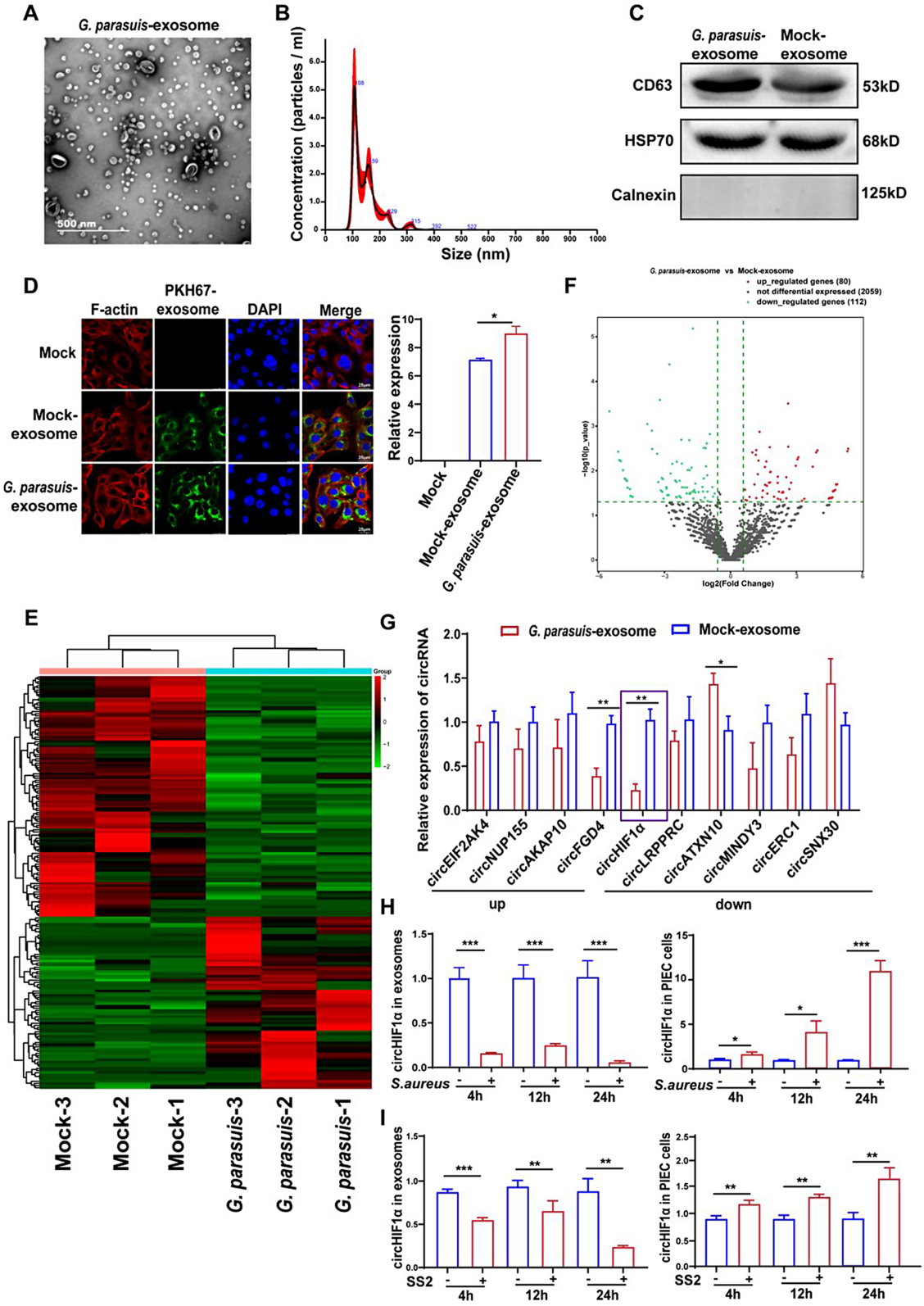

Fig. 1 (See legend on next page.)

(See figure on previous page.)

Fig. 1 Secretion of exosomes and selection of exosomal circHIF1α. **A** TEM was performed to confirm the shape of the exosomes isolated from the culture medium of PIEC cells infected with *G. parasuis*. Scale bar, 500 nm. **B** Exosome size distribution determined by nanoparticle tracking analysis (NTA) in the group of *G. parasuis* infection. **C** The expression of specific exosomal markers CD63, HSP70 and negative marker for exosome purity Calnexin by Western blot. **D** Transfer of exosomes between PIEC cells and PK-15 cells. The exosomes from PIEC cells were marked by PKH67 (green) and incubated with PK-15 cells, and the cytoskeleton of PK-15 cells was marked by F-actin (red). Afterward, IFA was performed for the detection of exosome distribution. Scale bar, 25 μm. Additionally, the relative fluorescence quantity of exosomes from different groups transferred into PK-15 cells was shown in the bar chart. **E** Heatmap showed differentially regulated circRNAs in exosomes isolated from the culture medium of PIEC cells infected with *G. parasuis* compared with that from normal PIEC cells. Red and green represent the upregulated and downregulated circRNAs, respectively. **F** Volcano plot of differentially expressed circRNAs in *G. parasuis*-exosomes and Mock-exosomes groups. **G** Selection and detection of different exosomal circRNAs from CircRNA sequencing by qRT-PCR. **H**–**I** The relative levels of circHIF1α in exosomes and precipitation of PIEC cells infected with *S. aureus* (**H**) or SS2 (**I**). Data are represented as mean ± SD. *$p<0.05$, **$p<0.01$, ***$p<0.001$

intraperitoneal injection, respectively. The infection dose of *G. parasuis* was 5×10^9 CFU, SS2 was 4×10^9 CFU, *S. aureus* was 7.5×10^9 CFU. At the same time, the exosome control group ($n=6$ mice/group) and circHIF1α control group ($n=6$ mice/group) without bacterial infection were established. The Clinical symptoms and mortality of mice were continuously observed for 14 d. The mice on the brink of death during the experiment and those still alive on the 14th d were euthanized. Different organs were fixed, embedded in paraffin, and sectioned. The sections were used for hematoxylin and eosin (H&E) staining. The bacterial content in different organs was determined by viable bacterial count and real-time PCR.

Data and statistical analysis

Statistical analyses were performed using GraphPad Prism 8.00 Software (GraphPad Software Inc., USA). Student's t-test (two-tailed) was employed when comparing between two groups. The Wilcoxon test and one-way ANOVA were used to compare measurement data among multiple groups. $p<0.05$ was considered statistically significant (*$p<0.05$, **$p<0.01$, ***$p<0.001$).

Results

Exosomes were taken up by PK-15 cells downstream after being secreted by upstream PIEC cells

We first determined whether PIEC cells infected with or without *G. parasuis* could secrete exosomes. The supernatants of PIEC cells infected with or without *G. parasuis* were collected to isolate exosomes. After isolation and purification from PIEC cells culture medium, morphological assessment with transmission electron microscopy was performed, and the result revealed the typical cup-shaped morphology of exosomes existed in the supernatants of PIEC cells infected with or without *G. parasuis* (Fig. 1A, and S1A). The NTA profile of exosomes revealed that most exosome particles had a diameter of 100 to 200 nm (Fig. 1B and S1B). The exosomal markers CD63, HSP70 and negative marker for exosome purity Calnexin were validated by Western blot analysis (Fig. 1C).

Next, we ascertained if the PK-15 cells had internalized these exosomes. Exosomes were labeled with the fluorescent dye PKH67 and added to the culture medium of PK-15 cells. After 12 h, there was green fluorescence staining in these cells, which suggested that exosomes were uptaken by PK-15 cells (Fig. 1D), and the fluorescence quantity of exosomes from PIEC cells infected with *G. parasuis* was higher than that without *G. parasuis* ($p<0.05$) (Fig. 1D).

Downregulated circHIF1α was encapsulated into exosomes from PIEC cells infected with bacteria

Firstly, we extracted exosomes from PIEC cells ($n=3$), and PIEC cells infected with *G. parasuis* ($n=3$), and circRNA sequencing was performed to examine their expression profiles. The cluster heatmap showed systemic expression differences in circRNAs $\log_2$CPM between the exosomes from PIEC cells infected with or without *G. parasuis* (Fig. 1E), and the scatter plot displayed the distribution of differential expression data (Fig. 1F). A total of 80 upregulated circRNAs and 112 downregulated circRNAs were screened (Data S1-S2). We analyzed the differentially upregulated circRNAs (Log2FC≥4.7, $P\leq0.0283$) and downregulated circRNAs (Log2FC≤-4.82, $P\leq0.015$) in the exosomes from PIEC cells infected with *G. parasuis.* 4 upregulated circRNAs and 6 downregulated circRNAs were further identified by qRT-PCR. Notably, chr1:190648252–190654424:+ (circRNA_ID) was the only circRNA to be validated with significantly downregulated expression in the exosomes from PIEC cells infected with *G. parasuis* compared with exosomes from uninfected PIEC cells (Fig. 1G), while the expression of this circRNA was upregulated expression in the precipitation from PIEC cells infected with *G. parasuis* (Fig. S1C). First, we designated circHIF1α, which is derived from HIF1α, as the sole circRNA that was found.

To determine whether the circHIF1α significant downregulation in exosomes from PIEC cells infected with *G. parasuis* was specific, the circHIF1α in exosomes and cell precipitation from PIEC cells infected with SS2 or *S. aureus* was also detected. The results showed that the circHIF1α in exosomes from PIEC cells infected with SS2 or *S. aureus* was significantly downregulated as well, while the circHIF1α was upregulated in PIEC cell precipitation (Fig. 1H-I).

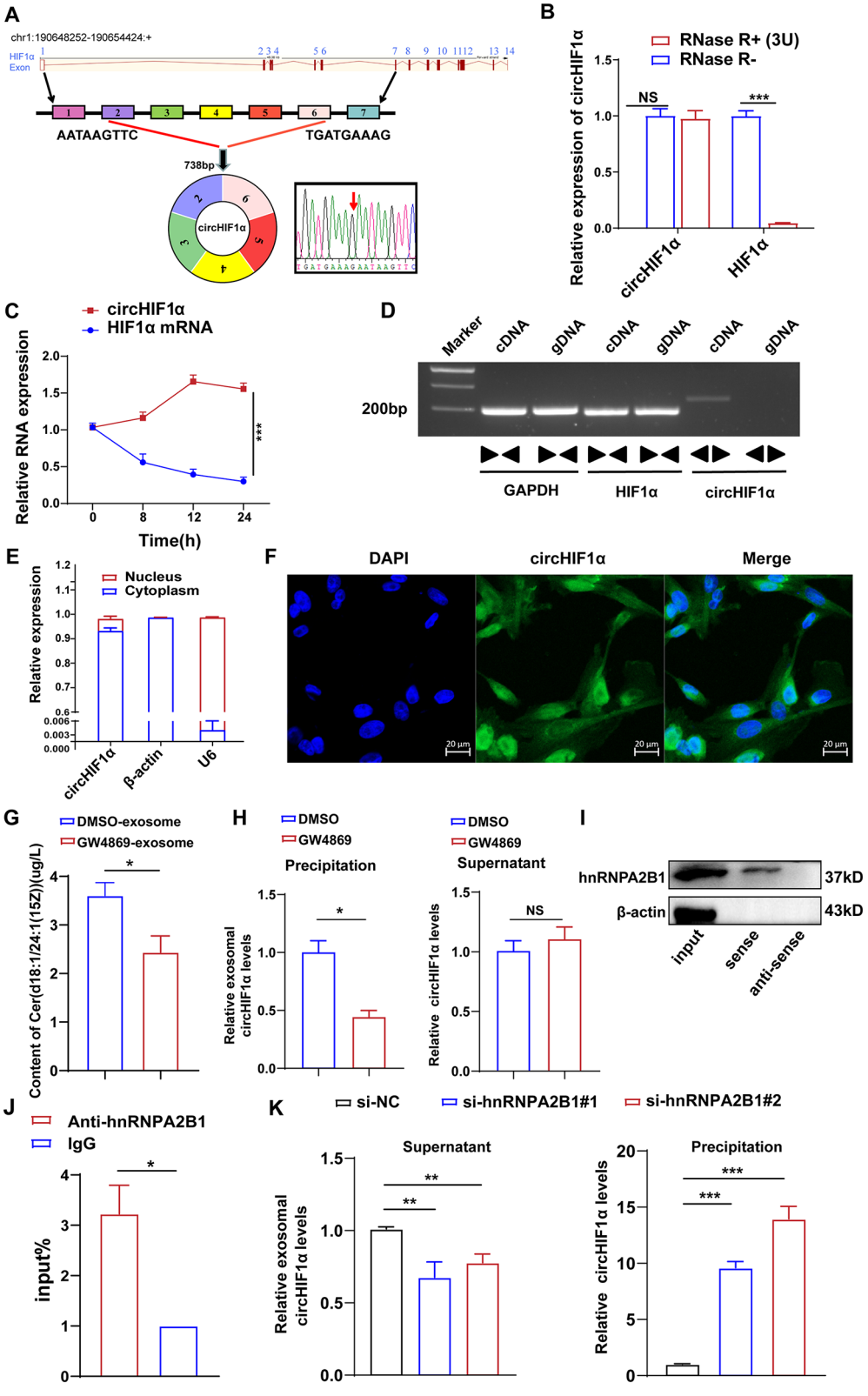

Fig. 2 (See legend on next page.)

(See figure on previous page.)

Fig. 2 Characterization of circHIF1α and hnRNPA2B1 mediates circHIF1α packaging into exosomes. **A** Schematic illustration of the genomic location and back-splicing junction site of circHIF1α via Sanger sequencing. **B** CircHIF1α and HIF1α mRNA levels in PIEC cells after RNase R digestion were detected by qRT-PCR. **C** The stability of circHIF1α and HIF1α mRNA in PIEC cells after actinomycin D treatment was evaluated. **D** The presence of circHIF1α and HIF1α mRNA in cDNA and gDNA from PIEC cells was detected by PCR with divergent and convergent primers and agarose gel electrophoresis analysis. **E** Cytoplasmic and nuclear fractionation indicated the distribution of circHIF1α in PIEC cells. β-actin and U6 were used as positive controls in the cytoplasm and nucleus, respectively. **F** The intracellular location of circHIF1α in PIEC cells was investigated with FISH. Scale bar, 20 μm. **G** C24:1 Ceramide Cer (d18:1/24:1(15Z)) content in exosome treated with 20μM GW4869 detected by High-performance LC/MS lipidomics analysis. **H** The level of circHIF1α in the precipitation of PIEC cells or exosomes isolated from the supernatants of PIEC cells treated with GW4869. **I** The interaction between circHIF1α and hnRNPA2B1 was detected by RNA pulldown assay. **J** RIP assay validated the bonding of circHIF1α and hnRNPA2B1. **K** The relative expression of circHIF1α in the precipitation or exosomes of PIEC cells after hnRNPA2B1 knockdown. Data are represented as mean ± SD. NS, not signifcant, $^{*}p < 0.05$, $^{**}p < 0.01$, $^{***}p < 0.001$

To summarize, our data suggested that circHIF1α was significantly downregulated in exosomes from PIEC cells infected with bacteria, and circHIF1α is a bona fide circRNA.

Characterization of exosomal circHIF1α in PIEC cells

CircHIF1α is generated from exons 2, 3, 4, 5 and 6 circularizations of HIF1α gene located on chr1 (190648252–190654424) and is 738 bp with a "head-to-tail" back-splice junction site (Fig. 2A), which was amplified using divergent primers and confirmed by Sanger sequencing (Fig. 2A). Moreover, we confirmed that circHIF1α expression was not significantly altered after treatment with RNase R and actinomycin D indicating an intact circular structure, while the expression of linear HIF1α was significantly downregulated (Fig. 2B-C). Furthermore, we designed specific divergent and convergent primers to amplify circHIF1α and its linear form. The results showed that circHIF1α was only amplified from cDNA, and no specific amplification products were observed using gDNA templates. In contrast, the linear form of HIF1α was amplified from both cDNA and gDNA by convergent primers (Fig. 2D). To verify further intracellular localization of circHIF1α, nuclear/cytoplasmic fractionation experiments, and FISH assays were performed, the results showed that circHIF1α was dominantly localized in the cytoplasm (Fig. 2E-F).

HnRNPA2B1 mediated circHIF1α packaging into exosomes of PIEC cells

To confirm the existence of circHIF1α in exosomes of PIEC cells, exosome formation was blocked by a pharmacological inhibitor of neutral sphingomyelinase-2 (nSMase) GW4869. High-performance LC/MS analysis showed that treatment with GW4869 decreased levels of Ceramide (d18:1/24:1(15Z)) in exosome of PIEC cells (Fig. 2G and S1D-E), and the result proved that the number of exosomes secreted by PIEC cells decreased after treatment with GW4869. At the same time, the level of exosomal circHIF1α was significantly inhibited, while did not affect the levels of circHIF1α in PIEC cells (Fig. 2H). In short, these results above clarified that the circHIF1α could be packaged into exosomes of PIEC cells.

Then, the mechanism of circHIF1α being packaged into exosomes was studied. We performed RNA pull-down and RIP assays to evaluate the interaction between circHIF1α and hnRNPA2B1 and found that they did interact with each other in PIEC cells (Fig. 2I-J and S1F). Moreover, circHIF1α expression was reduced in exosomes secreted from hnRNPA2B1-knockdown PIEC cells (Fig. 2K and S1G). In summary, these data suggested that circHIF1α could be packaged into exosomes of PIEC cells by hnRNPA2B1.

Exosomal circHIF1α from PIEC cells significantly increased the level of circHIF1α in PK-15 cells

We determined the effect of exosomal circHIF1α on the expression of circHIF1α in PK-15 cells through two experiments. Firstly, the transwell assay was used to simulate the effect of secreted exosomes on PK-15 cells after PIEC cells were infected with *G. parasuis* (Fig. S1H). The transwell assay demonstrated that exosomal circHIF1α from the culture medium of PIEC cells infected with *G. parasuis* reduced the expression levels of precipitation and supernatant of PK-15 cells (Fig. 3A-B). Secondly, circHIF1α overexpression plasmid (ov-circHIF1α) and siRNAs targeting circHIF1α were transfected into PIEC cells. We found that the expression levels of circHIF1α in exosomes and precipitation of PIEC cells were increased after circHIF1α overexpression (Fig. S1I-J), and the contrary results appeared in exosomes of PIEC cells when circHIF1α was knocked down (Fig. S1K). Moreover, the expression levels of circHIF1α in the precipitation of PK-15 cells increased when PK-15 cells were treated by the exosomes described above (Fig. 3C).

Exosomal circHIF1α significantly inhibited PK-15 cell proliferation in vitro

To explore the potential biological role of exosomal circHIF1α in the progression of PK-15 cells, circHIF1α overexpression plasmid and siRNAs targeting circHIF1α were transfected into PIEC cells, respectively, and the exosomes of PIEC cells were used to treat PK-15 cells. The results showed that the viability of PK-15 cells was significantly inhibited in the ov-circHIF1α group compared with the pLC5-ciR vector (ov-pLC5) group by

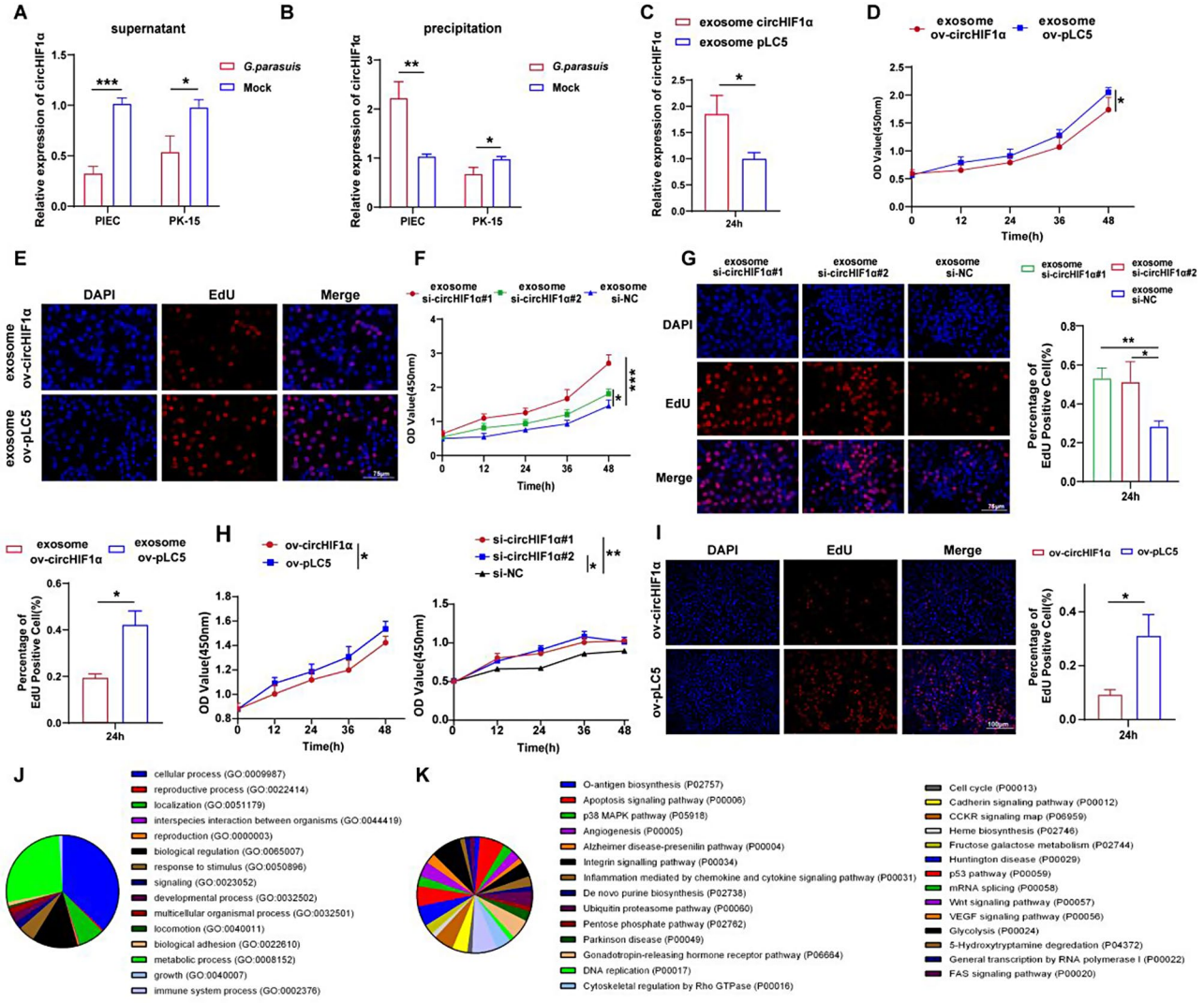

Fig. 3 Exosome and exosome-derived circHIF1α inhibits PK-15 cells proliferation. **A**–**B** The relative expression of circHIF1α in the precipitation or supernatant of PIEC/PK-15 cells after PIEC cells treated with *G. parasuis*. **C** The relative expression of circHIF1α in PK-15 cells treated with exosomes from overexpressed circHIF1α PIEC cells. **D**–**G** The proliferation of PK-15 cells treated with exosomes from PIEC cells after circHIF1α overexpression or knockdown was evaluated by CCK-8 (**D** and **F**) and EdU assay (**E** and **G**). Scale bar, 75 μm. **H**–**I**. The proliferation of PK-15 cells transfected with circHIF1α siRNA or overexpression vector was evaluated by CCK-8 (**H**) and EdU assay (**I**). Scale bar, 100 μm. **J** Mass spectrometric data of interaction between circHIF1α and ptotein showed the important correlated biological process. **K** The pathway result of mass spectrometry after RNA pulldown assay

CCK-8 and EdU assays (Fig. 3D and E), and contrary results were observed in the si-circHIF1α group (Fig. 3F and G).

In order to further accurately determine the function of the circHIF1α in the progression of PK-15 cells, circHIF1α overexpression plasmid and siRNAs targeting circHIF1α were directly transfected into PK-15 cells. The results displayed that the expression of circHIF1α was observably upregulated in PK-15 cells transfected with the circHIF1α overexpression vectors (Fig. S2A) and downregulated in PK-15 cells transfected with siRNAs by qRT-PCR (Fig. S2B). Moreover, CCK-8 and EdU assays showed that overexpression of circHIF1α significantly inhibited the viability of PK-15 cells (Fig. 3H-I), similar to the above results.

Exosomal circHIF1α promoted DNA damage and arrested the G1/S transition of the cell cycle in PK-15 cells

We first performed RNA pulldown assays, subsequent mass spectrometry assays, and GO enrichment analysis to predict the important correlated biological process and pathway with circHIF1α expression (Fig. 3J-K). As shown in Fig. 3J, the cellular process was significantly enriched in a large number of biological processes. In addition, Fig. 3K showed numerous signaling pathways involved in the regulation of cellular processes by

circHIF1α, including DNA replication, cell cycle and p53 pathway, and so on.

To assess the role of exosomal circHIF1α in PK-15 cell progression and DNA damage, the exosomes of PIEC cells after circHIF1α overexpression were used to treat PK-15 cells. We found that the amount of γ-H2AX fluorescence significantly increased in the exosome ov-circHIF1α group (Fig. 4A), while the contrary result was observed in the exosome si-circHIF1α group (Fig. 4B). In short, exosomal circHIF1α promoted the level of DNA damage. Considering that DNA damage affected the progression of the cell cycle, we determined cell cycle analysis by flow cytometry. The results revealed that the process of the cell cycle from the G1 phase to the S phase accelerated when circHIF1α in exosomes was inhibited (Fig. 4C).

According to Fig. 3K, we further investigated the function of circHIF1α in PK-15 cell progression and DNA damage. We detected the DNA damage-related proteins by Western blot, and the results showed that circHIF1α overexpression led to higher levels of γ-H2AX, NPM1, and p-p53 (Fig. 4D and S2C). In summary, the results showed that circHIF1α deteriorated DNA damage of PK-15 cells. Additionally, the results of flow cytometry revealed that upregulated circHIF1α led to a higher proportion of PK-15 cells in the G1 phase and a lower percentage of PK-15 cells in the S phase compared with the control group (Fig. 4E), indicating that circHIF1α overexpression caused G1/S arrest of PK-15 cells. Furthermore, the expression of related proteins in the G1/S phase was measured with Western blot, and it was found that CDK2, CDK4, Cyclin D1, and Cyclin E1 protein levels were significantly downregulated after overexpression of circHIF1α in PK-15 cells (Fig. 4F, and S2D), which could prevent cell cycle progression of PK-15 cells.

CircHIF1α inhibited bacterial invasion and adhesion to PK-15 cells by mediating DNA damage and arresting the G1/S phase

Previous data confirmed that circHIF1α inhibited the proliferation of PK-15 cells and caused DNA damage while leading to G1/S phase arrest. To clarify how overexpression of circHIF1α affects bacterial invasion and adhesion to PK-15 cells, the IF assay, bacteria adhesion, and invasion assays were performed. The results of the adhesion assay revealed that the adherence abilities of *G. parasuis* and *S. aureus* were significantly inhibited after overexpression of circHIF1α in PK-15 cells (Fig. 5A-B). In the invasion assays, the invasion abilities of PK-15 cells by *G. parasuis*, SS2 and *S. aureus* were markedly attenuated after overexpression of circHIF1α (Fig. 5A-C). The IF assay confirmed the above conclusions (Fig. 5D-F).

In order to further confirm whether DNA damage or G1/S phase inhibition would affect bacterial adhesion and invasion of bacteria to host cells, 250nM NSC 80,467 (Fig. S3A-B) or 2 mM Thymidine was used to treat the PK-15 cells after siRNAs targeting circHIF1α were transfected into PK-15 cells. The results of showed that the number of cells adhered to and invaded by bacteria decreased significantly after PK-15 cells were treated with NSC 80,467 (Fig. 5G-I) or Thymidine (Fig. 5J-L), which confirmed this conclusion about circHIF1α in inducing DNA damage and blocking G1/S transition phase to resist bacterial infection was valid.

CircHIF1α directly bound to IGF2BP3 protein in PK-15 cells

To explore the molecular mechanism of the circHIF1α-induced progression of PK-15 cells, we first performed RNA pulldown assays. The precipitates were detected via SDS-PAGE and silver staining (Fig. 6A). Subsequently, mass spectrometry (MS) analysis was used to explore potential proteins binding to circHIF1α. A total of 319 proteins were specifically identified in the precipitates of the circHIF1α probe, which did not include AGO2 (Data S3). Thus, circHIF1α could not perform functions as a ceRNA. Then, we intersected our mass spectrometry data with the RBPs predicted in the RBPmap database (http://rbpmap.technion.ac.il/) and RBPsuit database (http://www.csbio.sjtu.edu.cn/bioinf/RBPsuite/). Six proteins (NPM1, HNRNPM, PABPC1, HNRNPC, IGF2BP3, HNRNPUL2) were selected to detect by RNA pulldown and Western blot. The result validated that only IGF2BP3 existed in the precipitates of the circHIF1α probe (Fig. 6B and S3C). Moreover, the RIP assay with an IGF2BP3-specific antibody confirmed that IGF2BP3 could recruit circHIF1α (Fig. 6C and S3D). All the above results displayed that circHIF1α is directly bound to IGF2BP3 protein. Additionally, RNA FISH and IF analysis found that circHIF1α was colocalized with IGF2BP3 in the cytoplasm (Fig. 6D).

To explore the correlation between circHIF1α and IGF2BP3, PK-15 cells were transfected with ov-circHIF1α or si-circHIF1α and found that IGF2BP3 remarkably upregulated in PK-15 cells after overexpression of circHIF1α and significantly downregulated after knockdown of circHIF1α (Fig. 6E-F, and S3E-G). Further investigation showed that circHIF1α overexpression enhanced the protein expression levels of IGF2BP3 and extended the half-life of IGF2BP3 (Fig. 6G).

Knockdown of IGF2BP3 alleviated the proliferation inhibition caused by circHIF1α overexpression in vitro

To determine the effect of IGF2BP3 on the proliferation of PK-15 cells and verify the function of IGF2BP3 in the proliferation inhibition caused by circHIF1α overexpression, we performed CCK-8 and EdU assays. The data showed that IGF2BP3 knockdown dramatically reversed the effect of circHIF1α upregulation on cell proliferation

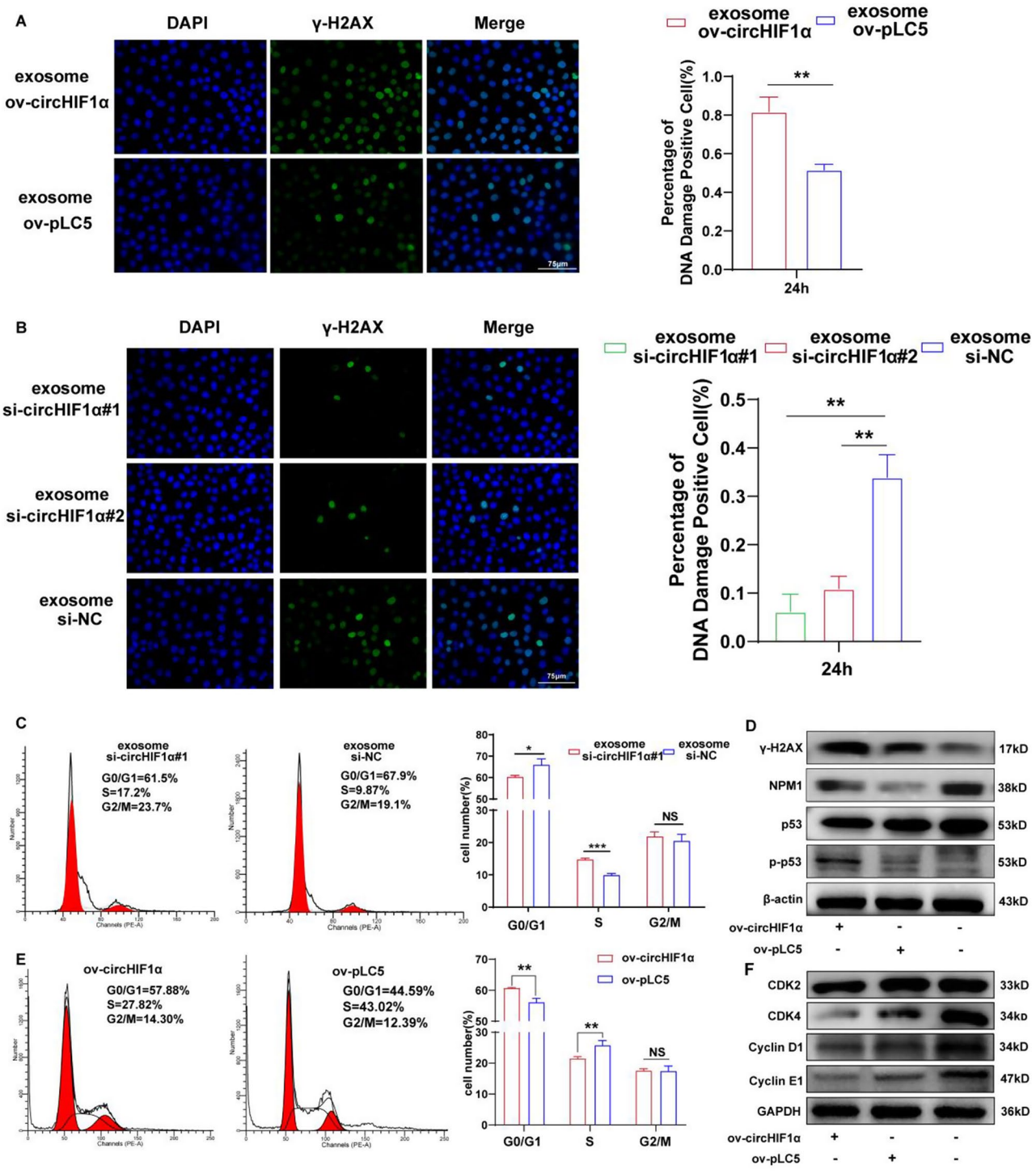

Fig. 4 Exosome and exosome-derived circHIF1α promotes PK-15 cells DNA damage, and mediates the G1/S phase. **A**–**B** The DNA damage level of PK-15 cells treated with exosomes from PIEC cells after circHIF1α overexpression or knockdown was detected by γ-H2AX immunofluorescence. Scale bar, 75 μm. **C** Cell cycle analysis was executed by flow cytometry when PK-15 cells were treated with exosomes from PIEC cells after circHIF1α knockdown. **D** Western blot showing the levels of DNA damage-related proteins, including γ-H2AX, NPM1, p53, and p-p53 in PK-15 cells transfected with ov-circHIF1α or ov-pLC5. **E** Cell cycle analysis was executed by flow cytometry after circHIF1α overexpression for 24 h. **F** The expression level of cell cycle-related proteins was detected in PK-15 cells after circHIF1α overexpression for 24 h by Western blot. Data are represented as mean ± SD. NS, not signifcant, *$p < 0.05$, **$p < 0.01$, ***$p < 0.001$

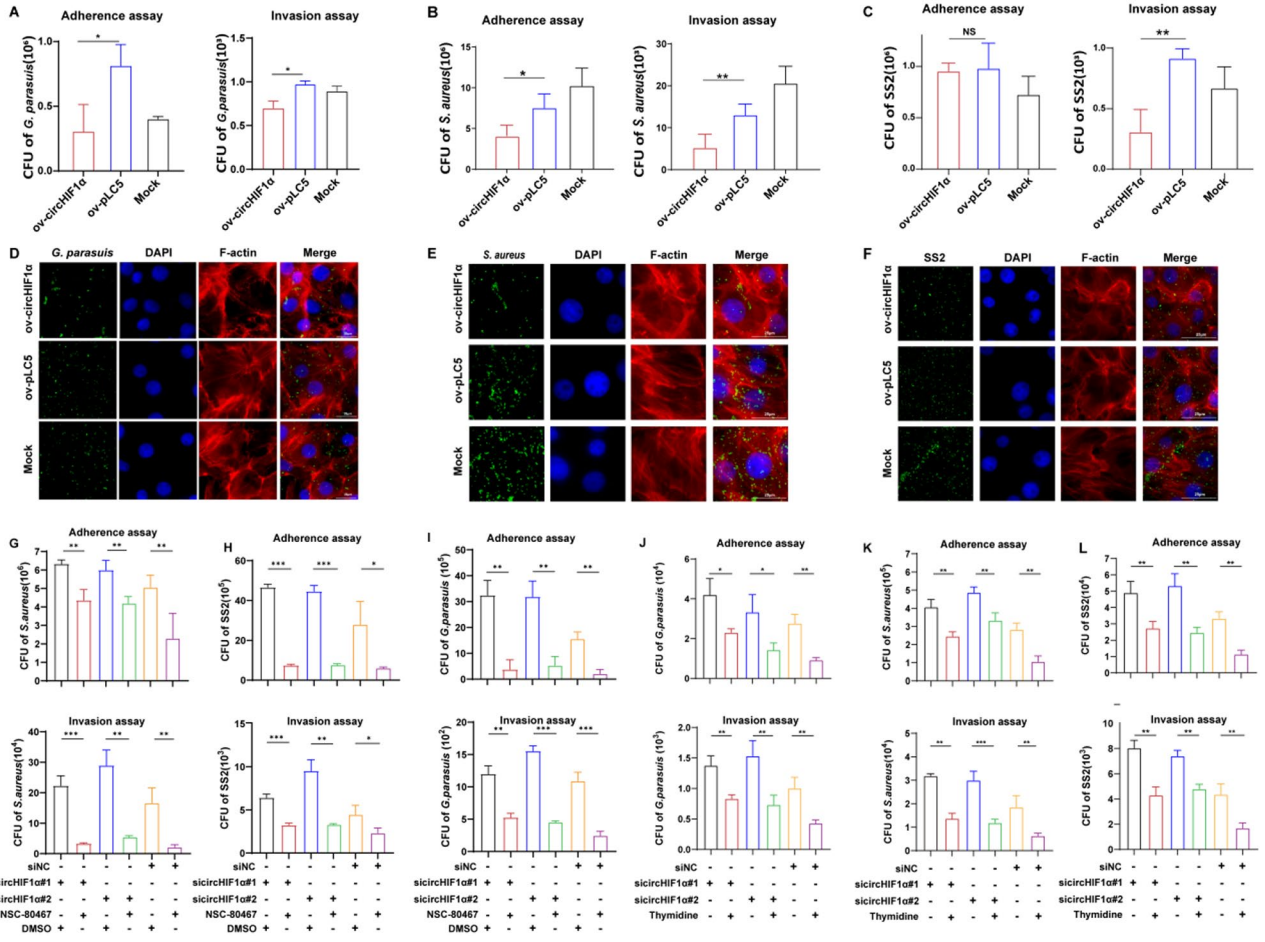

Fig. 5 CircHIF1α reduces bacterial adhesion and invasion for PK-15 cell. **A**–**C** The quantity of PK-15 cells infected with *G. parasuis* (**A**)/*S. aureus* (**B**)/SS2 (**C**) was identified by the viable counting method. **D**–**F** PK-15 cells infected with *G. parasuis*(**D**) /*S. aureus* (**E**)/SS2 (**F**) was identified by IF. Scale bar, 25 μm. **G**–**I** The quantity of PK-15 cells infected with *G. parasuis* (**G**) /*S. aureus* (**H**) /SS2 (**I**) was identified after PK-15 cells were treated with 250nM NSC 80,467 by bacteria adhesion and invasion assays. **J**–**L**. The quantity of PK-15 cells infected with *G. parasuis* (**J**), *S. aureus* (**K**), and SS2 (**L**) was identified after PK-15 cells were treated with 2mM Thymidine by bacteria adhesion and invasion assays. Data are represented as mean ± SD. NS, not signifcant, *$p < 0.05$, **$p < 0.01$, ***$p < 0.001$

in PK-15 cells (Fig. 6H-I). In contrast, the viability of PK-15 cell proliferation was enhanced when IGF2BP3 was downregulated in comparison with the control group (Fig. 6H-I).

CircHIF1α interacted with the K homology (KH) domain of IGF2BP3 in an m6A-mediated manner

We predicted the structure of IGF2BP3 using the Uniprot database (https://www.uniprot.org/) (Fig. 7A). Furtherly, according to the Uniprot database and NCBI database (https://www.ncbi.nlm.nih.gov/), we found that IGF2BP3 consisted of two domains, including RNA recognition motifs (RRMs) and K homology (KH). Therefore, we established three FLAG-tagged vectors to test which domain interacts with circHIF1α by RNA pulldown and Western blot (Fig. 7B-C, and Fig. S4A). The RIP-qPCR assay confirmed that circHIF1α mostly bound to the KH domain, indicating that KH domain was responsible for recruiting circHIF1α (Fig. 7D). To further investigate the motif necessary of circHIF1α for IGF2BP3 recruitment, the RNAfold WebServer database (http://rna.tbi.univie.ac.at//cgi-bin/RNAWebSuite/.

RNAfold.cgi) was used to predict the structure of the circHIF1α and divided it into two major sub-structure (Fig. 7E). As shown in Fig. S4A, two sub-structures of circHIF1α were established. RNA pulldown results showed that circHIF1α#2 mostly bound to IGF2BP3, and another sub-structure almost lost the binding capacity (Fig. 7F), confirming that 281–738 nt of circHIF1α were required for binding to IGF2BP3.

N6-methyladenosine (m6A) modifications regulate the RNA life cycle, RNA expression, and function [29, 30]. The previous research found that IGF2BP3 was the m6A reader [31]. Thus, MeRIP-qPCR assays demonstrated that circHIF1α was significantly enriched by an m6A antibody (Fig. 7G). To verify the m6A site of circHIF1α,

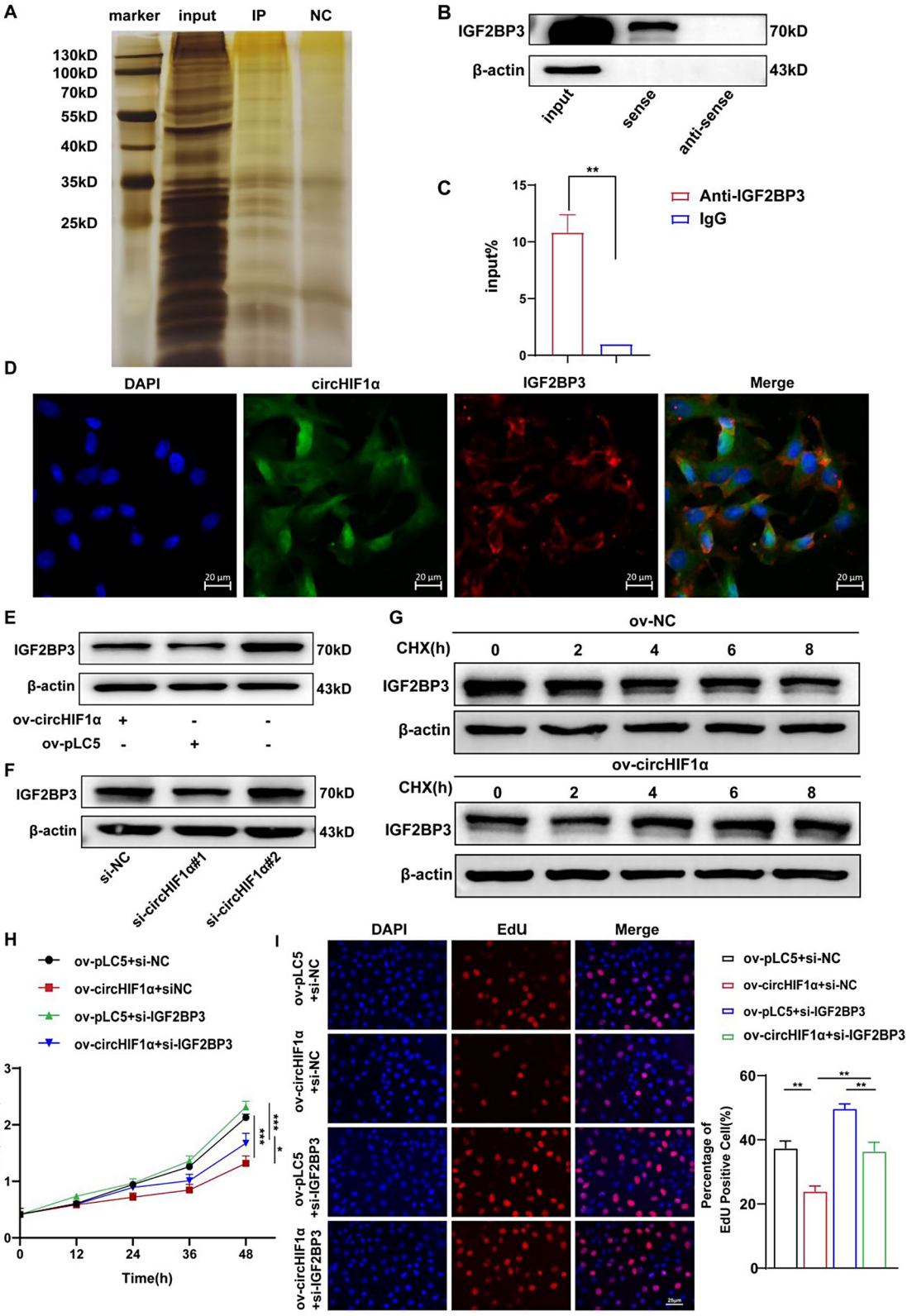

Fig. 6 (See legend on next page.)

(See figure on previous page.)

Fig. 6 CircHIF1α binds to IGF2BP3 to regulate the proliferation of PK-15 cells caused by circHIF1α. **A** RNA pulldown assay was performed using the specific biotin-labeled circHIF1α probe in PK-15 cell lysates, followed by silver staining. **B** RNA pulldown assay showed the interaction between circHIF1α and IGF2BP3 by Western blot. **C** RIP and qRT-PCR confirmed the enrichment of circHIF1α by IGF2BP3 in PK-15 cells using IGF2BP3 and IgG antibodies. **D** Immunofluorescence assessment of circHIF1α (green) and IFG2BP3 (red) colocalization in PK-15 cells. Scale bar, 20 μm. **E**–**F** The expression level of IGF2BP3 after overexpression (**E**) or knockdown (**F**) of circHIF1α via Western blot. **G** Western blot assays showed the protein levels of IGF2BP3 in PK-15 cells transfected with ov-circHIF1α or ov-NC, treated with 20 μg/mL CHX for the indicated periods. **H**–**I** The proliferation ability of PK-15 cells co-transfected with ov-circHIF1α, ov-pLC5, and si-IGF2BP3 was identified by CCK-8 (**H**) and EdU assays (**I**). Scale bar, 50 μm. Data are represented as mean ± SD. *$p < 0.05$, **$p < 0.01$, ***$p < 0.001$

we identified putative m6A motifs by the related database (http://www.cuilab.cn/m6asiteapp/result/HVX-69CpK7m/). As shown in Fig. S4B, there were 3 putative m6A motifs in the circHIF1α sequence, but only one was high confidence. Furthermore, we used a luciferase reporter containing firefly luciferase, followed by wild-type (WT) circHIF1α or mutant (MUT), where putative m6A sites were mutated (GAAC to GACC) (Fig. 7H). The result revealed that the luciferase activity of the WT reporter was significantly reduced compared with IGF2BP3 knockdown group, while the MUT reporter showed no significant difference (Fig. 7I). In summary, the site of 506 bp in circHIF1α was the main locus of m6A regulation, indicating that m6A modification of circHIF1α promoted its expression by enhancing its stability in an IGF2BP3-dependent manner.

IGF2BP3 affected cell progression through the RCC2 protein

The previous reports exhibited the direct interaction between IGF2BP3 and RCC2 and indicated that IGF2BP3 mediated the degradation of RCC2 mRNA by reading m6A-modified sites, and this regulation was m6A-dependent [32]. Furthermore, the downregulation of RCC2 caused greater DNA damage [33], and RCC2 played a role as a chromosomal passenger complex (CPC) implicated in all cell cycle phases [34]. In this study, we demonstrated the direct interaction between IGF2BP3 and RCC2 in PK-15 cells (Fig. 7J). In addition, IGF2BP3 knockdown enhanced the expression of RCC2 mRNA and protein (Fig. 7K-L), and a similar result was observed in the group of IGF2BP3 overexpression (ov-IGF2BP3) (Fig. 7M). To further evaluate whether RCC2 participated in the process of DNA damage, the Co-IP assay and IFA were performed. The results showed that RCC2 further mediated DNA damage through interaction with γ-H2AX (Fig. 7N-O).

Exosomal circHIF1α protected mice from bacterial infection

To determine whether exosomes could pass through blood circulation in vivo, we injected exosomes labeled with DiR through a mouse tail vein. After infection, we detected the fluorescence signal in mice at different times (Fig. 8A and S5A-B) and found that exosomes crossed blood circulation to other organs, and the fluorescence intensity reached the peak at 24 h after injection (Fig. 8A and S5A-B). The main target organs of exosomes were determined by the fluorescence intensity of different organs. There was a certain content of fluorescence in various organs, and the fluorescence in the liver was the strongest (Fig. 8B). Overall, our results showed that exosomes transported through blood circulation in vivo and traveled through blood vessels to different organs.

To further determine the role of exosomes or circHIF1α in protecting animals against bacterial infection, mice were challenged with *G. parasuis*, SS2 or *S. aureus*, respectively. The result showed that more than half of the bacteria-infected mice without treatment died, while the number of mice surviving was increased after treatment with exosomes or circHIF1α. Moreover, circHIF1α treatment had better protective effects on mice (Fig. 8C-E). Meanwhile, *G. parasuis* counts in different organs decreased significantly in the presence of exosome or circHIF1α, which showed comparable numbers in organs (Fig. 8F). Similar results were obtained when mice were infected with SS2 or *S. aureus* (Fig. 8G-H). Lastly, typical pathologic changes of the organs were alleviated in the treated groups as well (Fig. 8I and S5C-D). However, the organs showed hemorrhage and congestion after bacterial infection, especially in the spleen. At the same time, interstitial pneumonia also occurred in the bacteria-infected mice without treatment (Fig. 8I and S5C-D). In summary, circHIF1α played a protective role in bacterial infection in vivo.

Discussion

Exosomes produced from specific donor cells have been shown in more research to be able to transfer their cargo to recipient cells, where it may affect biological processes and cause a range of phenotypic alterations [15, 35]. In recent years, various studies have focused on exosomal circRNAs for their stability and the function of transferring substances between cells, and previous studies have verified that exosomal circRNAs participated in various types of tumors and human diseases [16, 36, 37]. However, whether exosomal circRNAs play critical roles in the process of bacterial infection remains elusive. Herein, we found that exosomes played an important role in intercellular communication between PIEC cells and PK-15 cells. A total of 112 downregulated circRNAs were identified in the exosomes from PEIC cells infected with *G. parasuis*.

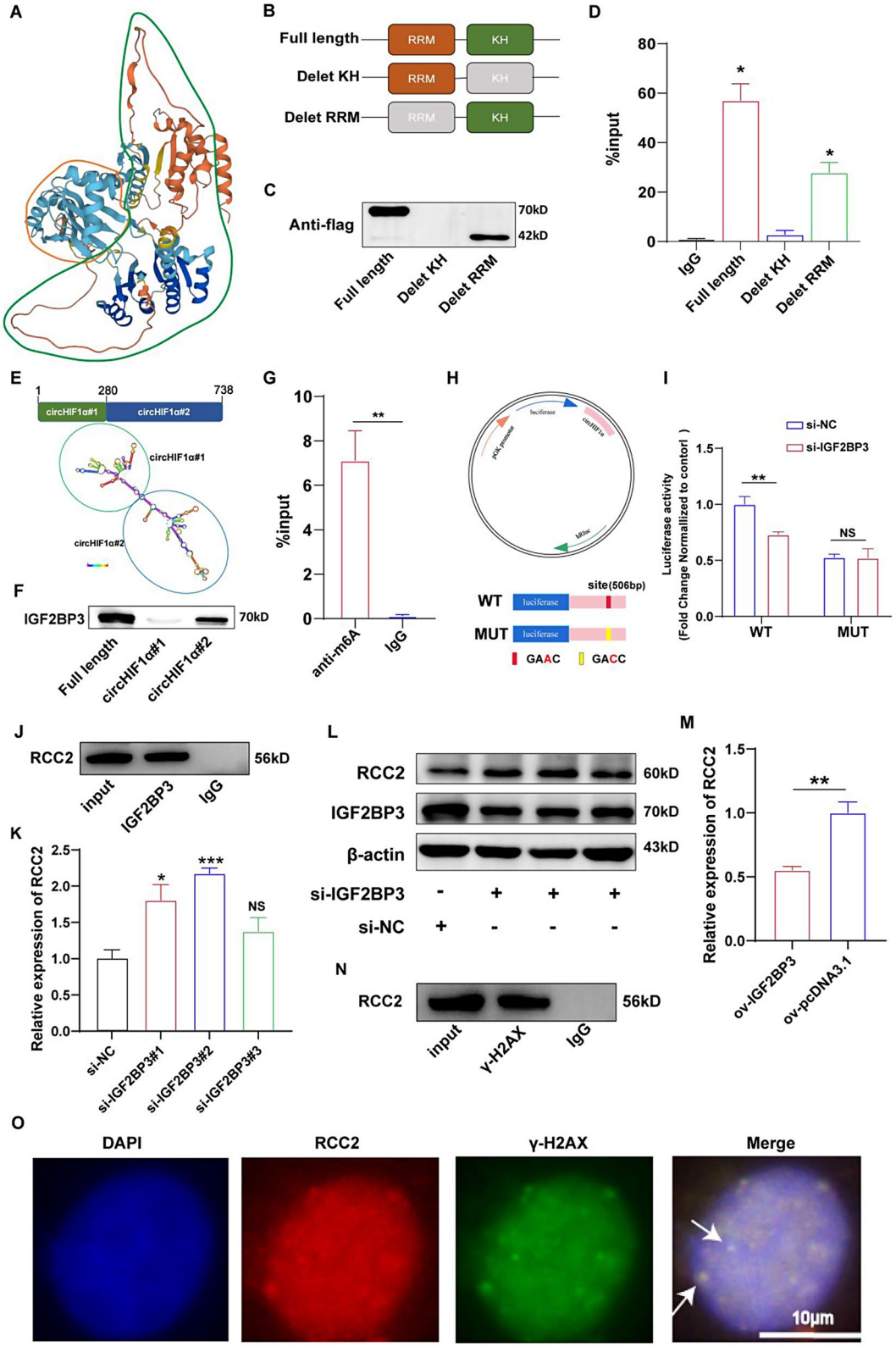

Fig. 7 (See legend on next page.)

(See figure on previous page.)

Fig. 7 CircHIF1α directly binds to the KH domain of IGF2BP3 protein in an m6A-mediated manner, and IGF2BP3 interacts with RCC2 in PK-15 cells to regulate the expression of γ-H2AX. **A** Structure of IGF2BP3 protein of *Sus scrofa* (pig), including RRM domain and KH domain. **B** Structural diagram of IGF2BP3 protein and two IGF2BP3 truncations (Delete KH or RRM). **C** RNA pulldown and Western blot assays showed the interaction site on IGF2BP3 with circHIF1α. **D** RIP and qRT-PCR analysis of circHIF1α enrichment pulldowns by IGF2BP3 antibody in PK-15 cells. **E** Secondary structure of circHIF1α predicted by the RNAfold WebServer and circHIF1α truncation site. **F** RNA pulldown and Western blot assays showed the interaction fragments on circHIF1α with IGF2BP3. **G** MeRIP assay confirmed that circHIF1α was highly enriched by the m6A antibody. **H** Schematic representation of the circHIF1α mutated (GAAC to GACC) firefly luciferase reporter vector. **I** Luciferase assays showed the main locus of m6A-mediated circHIF1α in PK-15 cells. **J** Co-IP assay showed the interaction between IGF2BP3 and RCC2. **K** The expression level of RCC2 after transfecting with si-IGF2BP3 or si-NC was detected by qRT-PCR. **L** The expression level of RCC2 after transfecting with si-IGF2BP3 or si-NC was detected by Western blot. **M** The expression level of RCC2 in ov-IGF2BP3 group or pcDNA3.1 vectors (ov-pcDNA3.1) group was detected by qRT-PCR. **N**–**O** The interaction between RCC2 and γ-H2AX was confirmed by Co-IP (**N**) and IF assay (**O**). Scale bar, 10 μm. Data are represented as mean ± SD. NS, not signifcant, $^{*}p < 0.05$, $^{**}p < 0.01$, $^{***}p < 0.001$

Of these, we first identified a novel circRNA derived from HIF1α gene, termed circHIF1α, which was remarkably downregulated. Notably, exosomal circHIF1α expression significantly decreased following Gram-negative bacterial infection, and Gram-positive bacterial infection corroborated the preceding findings, indicating that exosome circHIF1α decline is a typical event following bacterial infection. In contrast, treatment with GW4869, a specific pharmacological inhibitor of neutral sphingomyelinase-2 (nSMase) that blocks exosome production [28, 38], resulted in significant inhibition of circHIF1α in the cell culture medium. It's interesting to note that hnRNPA2B1 packaged circHIF1α into donor cell exosomes, which were then transferred to recipient cells and impacted cell division.

Interestingly, circHIF1α was packaged by hnRNPA2B1 into exosomes from donor cells, which were subsequently transported to recipient cells and affected cell division [15, 39, 40]. However, emerging evidence has indicated that some circRNAs are predominantly expressed in the cytoplasm to combine with RNA-binding proteins and regulate their activities [16, 41]. It was verified in this work that circHIF1α collaborates with IGF2BP3. Functionally, IGF2BP3 remarkably enhanced the inhibition of the proliferative capacity caused by circHIF1α overexpression of host cells. More specifically, the effect of circHIF1α overexpression on DNA damage and cell cycle was counteracted by IGF2BP3 downregulation in PK-15 cells. It has been reported that RCC2, the chromosome condensation 2 regulator, was a key protein for DNA damage [32], and Zhang et al. [42] expounded that IGF2BP3 promoted acute myeloid leukemia progression by enhancing RCC2 stability. Here, we further identified IGF2BP3 as a specific protein targeting the RCC2 protein, and RCC2 could cooperate with γ-H2AX to mediate DNA damage. Consequently, we have uncovered a new method by which IGF2BP3 contributes to DNA damage.

IGF2BP3 is an RBP and affects tumor progression [43, 44]. Still, there is more to learn about the relationship between circHIF1α and IGF2BP3. Our data demonstrated for the first time that the KH domain of IGF2BP3 was required for the association with 281–738 nt of circHIF1α in PK-15 cells. In recent years, the potential effects of m6A on circRNAs have attracted more attention [45], and IGF2BP3 is a well-known m6A-specific reader protein [46]. This work confirmed that IGF2BP3 combines the 506 bp region of circHIF1α in a m6A-mediated manner, suggesting that m6A alteration of circHIF1α enhanced its stability in a way that was dependent on IGF2BP3.

Numerous investigations revealed that the inflammatory reaction brought on by bacterial infection was associated with the bacteria's adherence and invasion of host cells as well as the impact of other cell phenotypes, such as the cell cycle, autophagy, apoptosis, and so on [47–49]. Moreover, the latest report showed that DNA damage could as an inducer of inflammation [50]. Therefore, we hypothesized that circHIF1α caused DNA damage and then induced an inflammatory response in the organism to resist bacterial infection. In this study, we focused on the functional mechanism of exosomal circRNAs in host cell progression and investigated their major roles in bacterial infection. Here, we uncovered a distinct mechanism that exosomal circHIF1α inhibited bacterial invasion and adhesion to host cells. Therefore, subsequent mass spectrometry and GO enrichment analysis were used to explore the functions of circHIF1α. The findings demonstrated their involvement in a wide range of biological functions, such as the p53 pathway, cell cycle, and DNA replication. Further research focused on DNA damage and cell cycle. We found that circHIF1α directly affected host cell proliferation by mediating DNA damage and modulating the G1/S transition of the cell cycle.

In our study, exosomes and circHIF1α are mainly located in multiple organs of mice, including the liver, spleen, lung, and so on. Furthermore, the death rate of mice due to bacterial infection was decreased by exosomes and circHIF1α, suggesting that these substances inhibited bacterial invasion and shielded the organism from bacterial infection. Moreover, the protective rate of circHIF1α was higher than that of exosomes, probably because exosomes contained complex components, including DNA and some bacterial proteins.

However, there were still some limitations existed in our study. Although we revealed a partial association between exosomal circHIF1α and cell proliferation,

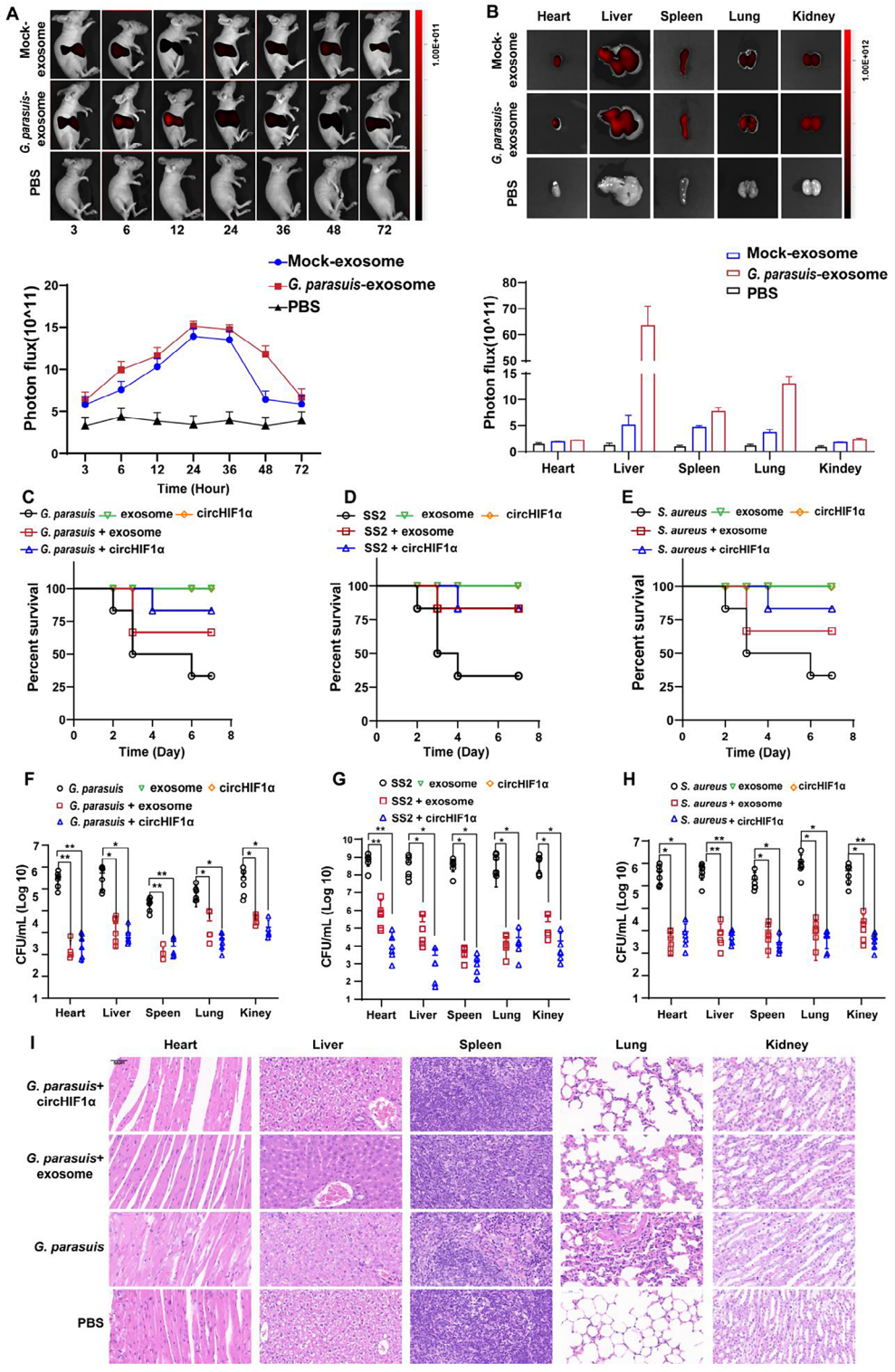

Fig. 8 Exosomal circHIF1α resists bacterial infection in vivo. **A** Left, Bioluminescent image showed localization of *G. parasuis*-exosome (20 mg/kg) or Mock-exosome (20 mg/kg) in mice after injecting through the tail vein at different times. Right, the fluorescence intensity of exosomes in vivo. $n = 6$ mice/group. **B** The fluorescence intensity of *G. parasuis*-exosome (20 mg/kg) or Mock-exosome (20 mg/kg) in different organs of mice. $n = 6$ mice/group. **C**–**E** The effect of exosomes and circHIF1α on the survival of mice after *G. parasuis* (**C**)/SS2 (**D**)/*S. aureus* (**E**) infection. $n = 6$ mice/group. **F**–**H** The effect of exosomes and circHIF1α on *G. parasuis* (**F**)/SS2 (**G**)/*S. aureus* (**H**) count of different organs after mice were infected with *G. parasuis*. **I** H&E staining of various organs after mice were infected with *G. parasuis* followed treating with exosome or circHIF1α. Scale bar, 50 μm. $n = 6$ mice/group. Data are represented as mean ± SD. $^{*}p < 0.05$, $^{**}p < 0.01$

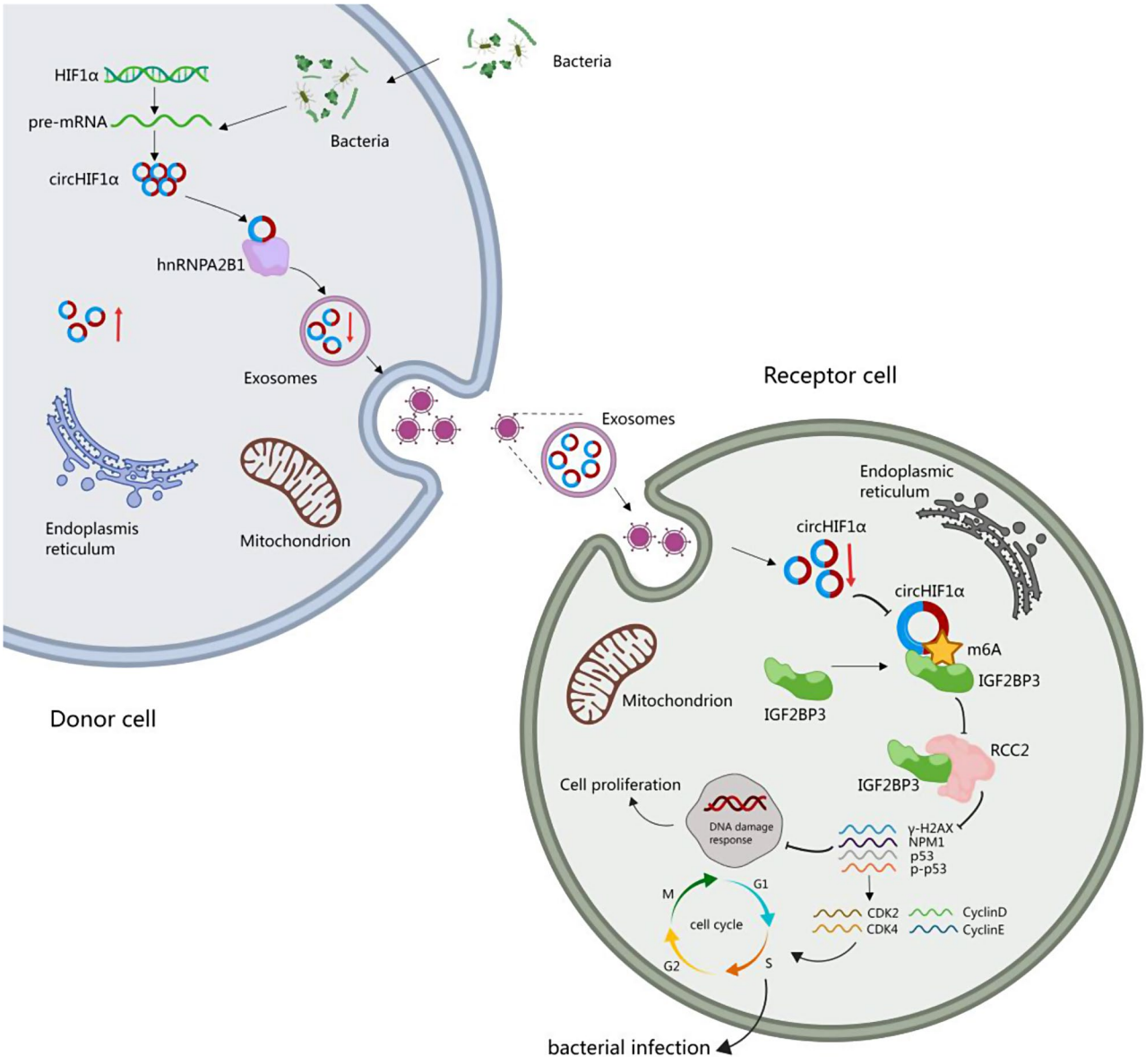

Fig. 9 Proposed model for the potential function of exosomal circHIF1α in bacterial infection progression

expounding that exosomal circHIF1α protected the organism against bacterial infection, whether circRNA affects the lysosome function of host cells after bacterial infection and then influenced the degradation process of bacteria still requires further investigation. In the meantime, we discovered that the precipitate of PIEC cells had an increased level of circHIF1α; the cause of this phenomenon will require more investigation in the near future.

This study discovered a new circHIF1α that was downregulated in exosomes derived from bacterially infected PIEC cells and packaged into exosomes by hnRNPA2B1. This association was made for the first time with a pathogenic bacterial infection. Moreover, exosomal circHIF1α secreted by PIEC cells could be taken up in PK-15 cells and had direct effects on cell proliferation. Mechanistically, circHIF1α interacted with KH domain of IGF2BP3 in an m6A-mediated manner and mediated the interaction between RCC2 and γ-H2AX, which remarkably suppressed bacterial infection to host cells and organisms by mediating DNA damage and modulating G1/S transition of cell cycle (Fig. 9). As a result, this study offered a new therapeutic target for bacterial infection in addition to reporting a novel method of exosomal circRNA against pathogenic bacteria attack.

Supplementary Information

The online version contains supplementary material available at https://doi.org/10.1186/s12951-024-02932-4.

Supplementary Material 1

Supplementary Material 2

Supplementary Material 3

Supplementary Material 4

Acknowledgements
This study was supported by the National Key Research and Development Program of China (2022YFD1800905), Natural Science Funds of Shandong Province (ZR2022MC002), Key R&D Program of Shandong Province, China (2022CXPT010), Shandong Provincial Modern Agricultural Industry and Technology System (SDAIT-08), New high schools 20 in Jinan of Shandong Province (202333065), and the Taishan Scholars Program.

Author contributions
J.Y. and J. W. provided the conceptual idea and designed the study. Y. G., F. L., S. R., J. Y., J. J. and G. F. carried out the study and acquired the data. Y. Z., J. L., L.D., Z. C., and W. S. analyzed and interpreted the data. J. Y. and Y. G. wrote the manuscript. J. Y., Y. G., F. L., Y. Z., and J. W. performed the manuscript revision. Y. G. and F. L. prepared the manuscript for submission. J. Y. and J. W. supervised the study. All authors have read and agreed to the published version of the manuscript.

Data availability
No datasets were generated or analysed during the current study.

Declarations

Competing interests
The authors declare no competing interests.

Author details
[1]Key Laboratory of Livestock and Poultry Multi-omics of MARA, Instihte of Animal Science and veterinary Medicine, Shandong Academy of Agricultural Sciences, Jinan 250100, P. R. China
[2]School of Life Sciences, Shandong Normal University, Jinan 250014, China

Received: 23 July 2024 / Accepted: 13 October 2024
Published online: 24 October 2024

References

1. Deusenbery C, Wang Y, Shukla A. Recent innovations in bacterial infection detection and treatment. ACS Infect Dis. 2021;7(4):695–720.
2. Xu Z, Chen B, Zhang Q, Liu L, Zhang A, Yang Y, Huang K, Yan S, Yu J, Sun X, Jin M. *Streptococcus suis 2* Transcriptional Regulatorstimulatesulates Cytokine Production and Bacterempromoterstreptococcalctoxic shock likek-Like Syndrome. Front Microbiol. 2018;9:1309.
3. Abraham L, Bamberger DM. *Staphylococcus aureus* Bacteremia: Contemporary Management. Mo Med. 2020;117(4):341–5.
4. Luo X, Chang X, Zhou H, Lin H, Fan H. *Glaesserella parasuis* induces inflammatory response in 3D4/21 cells through activation of NLRP3 inflammasome signaling pathway via ROS. Vet Microbiol. 2021;256:109057.
5. Tinévez C, Velardo F, Ranc AG, Dubois D, Pailhoriès H, Codde C, Join-Lambert O, Gras E, Corvec S, Neuwirth C, Melenotte C, Dorel M, Lagneaux AS, Pichon M, Doat V, Fournier D, Lemaignen A, Bouard L, Patoz P, Hery-Arnaud G, Lemaitre N, Couzigou C, Guillard T, Recalt E, Bille E, Belaroussi Y, Neau D, Cazanave C, Lehours P, Puges M. Campylobacteremia study group. Retrospective multicentric study on Campylobacter Spp. Bacteremia in France: the Campylobacteremia Study. Clin Infect Dis. 2022;75(4):702–9.
6. Kalluri R, LeBleu VS. The biology, function, and biomedical applications of exosomes. Science. 2020;367(6478):eaau6977.
7. Liu DA, Tao K, Wu B, Yu Z, Szczepaniak M, Rames M, Yang C, Svitkina T, Zhu Y, Xu F, Nan X, Guo W. A phosphoinositide switch mediates exocyst recruitment to multivesicular endosomes for exosome secretion. Nat Commun. 2023;14(1):6883.
8. Arya SB, Collie SP, Parent CA. The ins-and-outs of exosome biogenesis, secretion, and internalization. Trends Cell Biol. 2024;34(2):90–108.
9. Zhang L, Yu D. Exosomes in cancer development, metastasis, and immunity. Biochim Biophys Acta Rev Cancer. 2019;1871(2):455–68.
10. Tong X, Dang X, Liu D, Wang N, Li M, Han J, Zhao J, Wang Y, Huang M, Yang Y, Yang Y, Wang W, Kou Y, Kou J. Exosome-derived circ_0001785 delays atherogenesis through the ceRNA network mechanism of miR-513a-5p/TGFBR3. J Nanobiotechnol. 2023;21(1):362.
11. Kristensen LS, Andersen MS, Stagsted LVW, Ebbesen KK, Hansen TB, Kjems J. The biogenesis, biology and characterization of circular RNAs. Nat Rev Genet. 2019;20(11):675–91.
12. Wang J, Zhao X, Wang Y, Ren F, Sun D, Yan Y, Kong X, Bu J, Liu M, Xu S. circRNA-002178 act as a ceRNA to promote PDL1/PD1 expression in lung adenocarcinoma. Cell Death Dis. 2020;11(1):32.
13. Mao G, Xu Y, Long D, Sun H, Li H, Xin R, Zhang Z, Li Z, Yang Z, Kang Y. Exosome-transported circRNA_0001236 enhances chondrogenesis and suppress cartilage degradation via the miR-3677-3p/Sox9 axis. Stem Cell Res Ther. 2021;12(1):389.
14. Pan Z, Zhao R, Li B, Qi Y, Qiu W, Guo Q, Zhang S, Zhao S, Xu H, Li M, Gao Z, Fan Y, Xu J, Wang H, Wang S, Qiu J, Wang Q, Guo X, Deng L, Zhang P, Xue H, Li G. EWSR1-induced circNEIL3 promotes glioma progression and exosome-mediated macrophage immunosuppressive polarization via stabilizing IGF2BP3. Mol Cancer. 2022;21(1):16.
15. Wang L, Wu X, Ruan Y, Zhang X, Zhou X. Exosome-transmitted hsa_circ_0012634 suppresses pancreatic ductal adenocarcinoma progression through regulating miR-147b/HIPK2 axis. Cancer Biol Ther. 2023;24(1):2218514.
16. Zheng R, Zhang K, Tan S, Gao F, Zhang Y, Xu W, Wang H, Gu D, Zhu L, Li S, Chu H, Zhang Z, Liu L, Du M, Wang M. Exosomal circLPAR1 functions in colorectal cancer diagnosis and tumorigenesis through suppressing BRD4 via METTL3-eIF3h interaction. Mol Cancer. 2022;21(1):49.
17. Deng X, Su R, Weng H, Huang H, Li Z, Chen J. RNA N^6-methyladenosine modification in cancers: current status and perspectives. Cell Res. 2018;28(5):507–17.
18. Chen Y, Lin Y, Shu Y, He J, Gao W. Interaction between N6-methyladenosine (m6A) modification and noncoding RNAs in cancer. Mol Cancer. 2020;19(1):94.
19. Zhong C, Long Z, Yang T, Wang S, Zhong W, Hu F, Teoh JY, Lu J, Mao X. M6A-modified circRBM33 promotes prostate cancer progression via PDHA1-mediated mitochondrial respiration regulation and presents a potential target for ARSI therapy. Int J Biol Sci. 2023;19(5):1543–63.
20. Chen RX, Chen X, Xia LP, Zhang JX, Pan ZZ, Ma XD, Han K, Chen JW, Judde JG, Deas O, Wang F, Ma NF, Guan X, Yun JP, Wang FW, Xu RH. Dan Xie. N^6-methyladenosine modification of circNSUN2 facilitates cytoplasmic export and stabilizes HMGA2 to promote colorectal liver metastasis. Nat Commun. 2019;10(1):4695.
21. Liu H, Lan T, Li H, Xu L, Chen X, Liao H, Chen X, Du J, Cai Y, Wang J, Li X, Huang J, Yuan K, Zeng Y. Circular RNA circDLC1 inhibits MMP1-mediated liver cancer progression via interaction with HuR. Theranostics. 2021;11(3):1396–411.
22. Chen Y, Pan C, Wang X, Xu D, Ma Y, Hu J, Chen P, Xiang Z, Rao Q, Han X. Silencing of METTL3 effectively hinders invasion and metastasis of prostate cancer cells. Theranostics. 2021;11(16):7640–57.
23. Liang L, Zhu Y, Li J, Zeng J, Wu L. ALKBH5-mediated m6A modification of circCCDC134 facilitates cervical cancer metastasis by enhancing HIF1A transcription. J Exp Clin Cancer Res. 2022;41(1):261.
24. Li B, Zhao R, Qiu W, Pan Z, Zhao S, Qi Y, Qiu J, Zhang S, Guo Q, Fan Y, Xu H, Li M, Li G, Xue H. The N^6-methyladenosine-mediated lncRNA WEE2-AS1 promotes glioblastoma progression by stabilizing RPN2. Theranostics. 2022;12(14):6363–79.
25. Lai JJ, Chau ZL, Chen SY, Hill JJ, Korpany KV, Liang NW, Lin LH, Lin YH, Liu JK, Liu YC, Lunde R, Shen WT. Exosome Processing and characterization approaches for Research and Technology Development. Adv Sci. 2022;9(15):e2103222.
26. Hui B, Zhou C, Xu Y, Wang R, Dong Y, Zhou Y, Ding J, Zhang X, Xu J, Gu Y. Exosomes secreted by Fusobacterium nucleatum-infected colon cancer cells transmit resistance to oxaliplatin and 5-FU by delivering hsa_circ_0004085. J Nanobiotechnol. 2024;22(1):62.
27. Fan Z, Xiao K, Lin J, Liao Y, Huang X. Functionalized DNA enables programming Exosomes/Vesicles for Tumor Imaging and Therapy. Small. 2019;15(47):e1903761.
28. Peche VS, Pietka TA, Jacome-Sosa M, Samovski D, Palacios H, Chatterjee-Basu G, Dudley AC, Beatty W, Meyer GA, Goldberg IJ, Abumrad NA. Endothelial cell

CD36 regulates membrane ceramide formation, exosome fatty acid transfer and circulating fatty acid levels. Nat Commun. 2023;14(1):4029.
29. Zaccara S, Ries RJ, Jaffrey SR. Reading, writing and erasing mRNA methylation. Nat Rev Mol Cell Biol. 2019;20(10):608–24.
30. Livneh I, Moshitch-Moshkovitz S, Amariglio N, Rechavi G, Dominissini D. The m^6A epitranscriptome: transcriptome plasticity in brain development and function. Nat Rev Neurosci. 2020;21(1):36–51.
31. Yang L, Yan B, Qu L, Ren J, Li Q, Wang J, Kan X, Liu M, Wang Y, Sun Y, Wang C, Wang P. IGF2BP3 regulates TMA7-mediated Autophagy and Cisplatin Resistance in Laryngeal Cancer via m6A RNA methylation. Int J Biol Sci. 2023;19(5):1382–400.
32. Zhang N, Shen Y, Li H, Chen Y, Zhang P, Lou S, Deng J. The m6A reader IGF2BP3 promotes acute myeloid leukemia progression by enhancing RCC2 stability. Exp Mol Med. 2022;54(2):194–205.
33. Xu X, Zhou X, Zhang J, Li H, Cao Y, Tan X, Zhu X, Yang J. MicroRNA-191 modulates cisplatin-induced DNA damage response by targeting RCC2. FASEB J. 2020;34(10):13573–85.
34. Guo K, Zhao C, Lang B, Wang H, Zheng H, Zhang F. Regulator of chromosome condensation 2 modulates cell cycle progression, Tumorigenesis, and Therapeutic Resistance. Front Mol Biosci. 2021;7:620973.
35. van Niel G, D'Angelo G, Raposo G. Shedding light on the cell biology of extracellular vesicles. Nat Rev Mol Cell Biol. 2018;19(4):213–28.
36. Li Q, Xu M, Zhang Z, Yin M, Zhang Y, Liu F. Urinary exosomal hsa_circ_0001250 as a novel diagnostic biomarker of idiopathic membranous nephropathy. J Transl Med. 2022;20(1):607.
37. Li G, Lan Q. Exosome-mediated transfer of circ-GLIS3 enhances Temozolomide Resistance in Glioma cells through the miR-548m/MED31 Axis. Cancer Biother Radiopharm. 2023;38(1):62–73.
38. Catalano M, O'Driscoll L. Inhibiting extracellular vesicles formation and release: a review of EV inhibitors. J Extracell Vesicles. 2019;9(1):1703244.
39. Luo C, Zhao X, Wang Y, Li Y, Wang T, Li S. A novel circ_0000654/miR-375/E2F3 ceRNA network in esophageal squamous cell carcinoma. Thorac Cancer. 2022;13(15):2223–34.
40. Hu Z, Chen G, Zhao Y, Gao H, Li L, Yin Y, Jiang J, Wang L, Mang Y, Gao Y, Zhang S, Ran J, Li L. Exosome-derived circCCAR1 promotes CD8 + T-cell dysfunction and anti-PD1 resistance in hepatocellular carcinoma. Mol Cancer. 2023;22(1):55.
41. Yang R, Chen H, Xing L, Wang B, Hu M, Ou X, Chen H, Deng Y, Liu D, Jiang R, Chen J. Hypoxia-induced circWSB1 promotes breast cancer progression through destabilizing p53 by interacting with USP10. Mol Cancer. 2022;21(1):88.
42. Zheng R, Du M, Wang X, Xu W, Liang J, Wang W, Lv Q, Qin C, Chu H, Wang M, Yuan L, Qian J, Zhang Z. Exosome-transmitted long non-coding RNA PTENP1 suppresses bladder cancer progression. Mol Cancer. 2018;17(1):143.
43. Yang F, Ma Q, Huang B, Wang X, Pan X, Yu T, Ran L, Jiang S, Li H, Chen Y, Liu Y, Liang C, Ren J, Zhang Y, Wang S, Li W, Xiao B. CircNFATC3 promotes the proliferation of gastric cancer through binding to IGF2BP3 and restricting its ubiquitination to enhance CCND1 mRNA stability. J Transl Med. 2023;21(1):402.
44. Dixit D, Prager BC, Gimple RC, Poh HX, Wang Y, Wu Q, Qiu Z, Kidwell RL, Kim LJY, Xie Q, Vitting-Seerup K, Bhargava S, Dong Z, Jiang L, Zhu Z, Hamerlik P, Jaffrey SR, Zhao JC, Wang X, Rich JN. The RNA m6A reader YTHDF2 maintains Oncogene expression and is a targetable dependency in Glioblastoma Stem cells. Cancer Discov. 2021;11(2):480–99.
45. Tang C, Xie Y, Yu T, Liu N, Wang Z, Woolsey RJ, Tang Y, Zhang X, Qin W, Zhang Y, Song G, Zheng W, Wang J, Chen W, Wei X, Xie Z, Klukovich R, Zheng H, Quilici DR, Yan W. m^6A-dependent biogenesis of circular RNAs in male germ cells. Cell Res. 2020;30(3):211–28.
46. Huang H, Weng H, Sun W, Qin X, Shi H, Wu H, Zhao BS, Mesquita A, Liu C, Yuan CL, Hu YC, Hüttelmaier S, Skibbe JR, Su R, Deng X, Dong L, Sun M, Li C, Nachtergaele S, Wang Y, Hu C, Ferchen K, Greis KD, Jiang X, Wei M, Qu L, Guan JL, He C, Yang J, Chen J. Recognition of RNA N6-methyladenosine by IGF2BP proteins enhances mRNA stability and translation. Nat Cell Biol. 2018;20(3):285–295.
47. Xie F, Chen R, Zhao J, Xu C, Zan C, Yue B, Tian W, Yi W. Cell cycle kinase CHEK2 in macrophages alleviates the inflammatory response to Staphylococcus aureus-induced pneumonia. Exp Lung Res. 2022;48(2):53–60.
48. Wang S, Wang G, Tang YD, Li S, Qin L, Wang M, Yang YB, Gottschalk M, Cai X. Streptococcus suis serotype 2 infection induces splenomegaly with Splenocyte apoptosis. Microbiol Spectr. 2022;10(6):e0321022.
49. Liu M, Wang Q, Wu W, Chen M, Zhang P, Guo M, Lin H, Ma Z, Zhou H, Fan H. Glaesserella parasuis serotype 5 breaches the porcine respiratory epithelial barrier by inducing autophagy and blocking the cell membrane Claudin-1 replenishment. PLoS Pathog. 2022;18(10):e1010912.
50. Zhao Y, Simon M, Seluanov A, Gorbunova V. DNA damage and repair in age-related inflammation. Nat Rev Immunol. 2023;23(2):75–89.

Publisher's note